暗黒物質アクシオンを始めとする, Wave-like dark matter の実験的探索

東北大学 ニュートリノ科学研究センター
岸本 康宏

ICEPPシンポジウム

2023年2月19日

Dark matter in various scale

Small scale → **Large scale**

銀河の回転速度

衝突する銀河

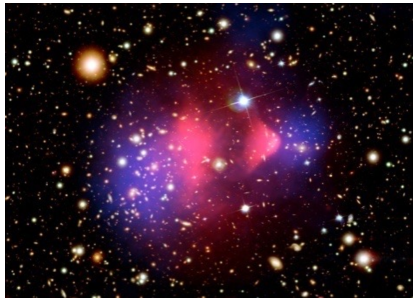

暗黒物質地図

銀河大規模構造

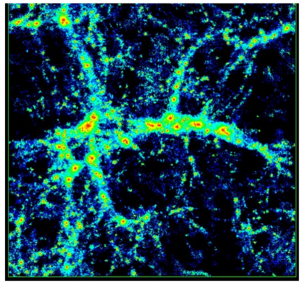

宇宙背景輻射

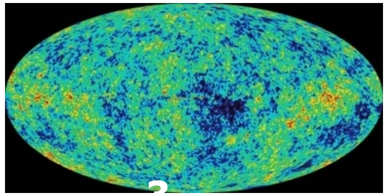

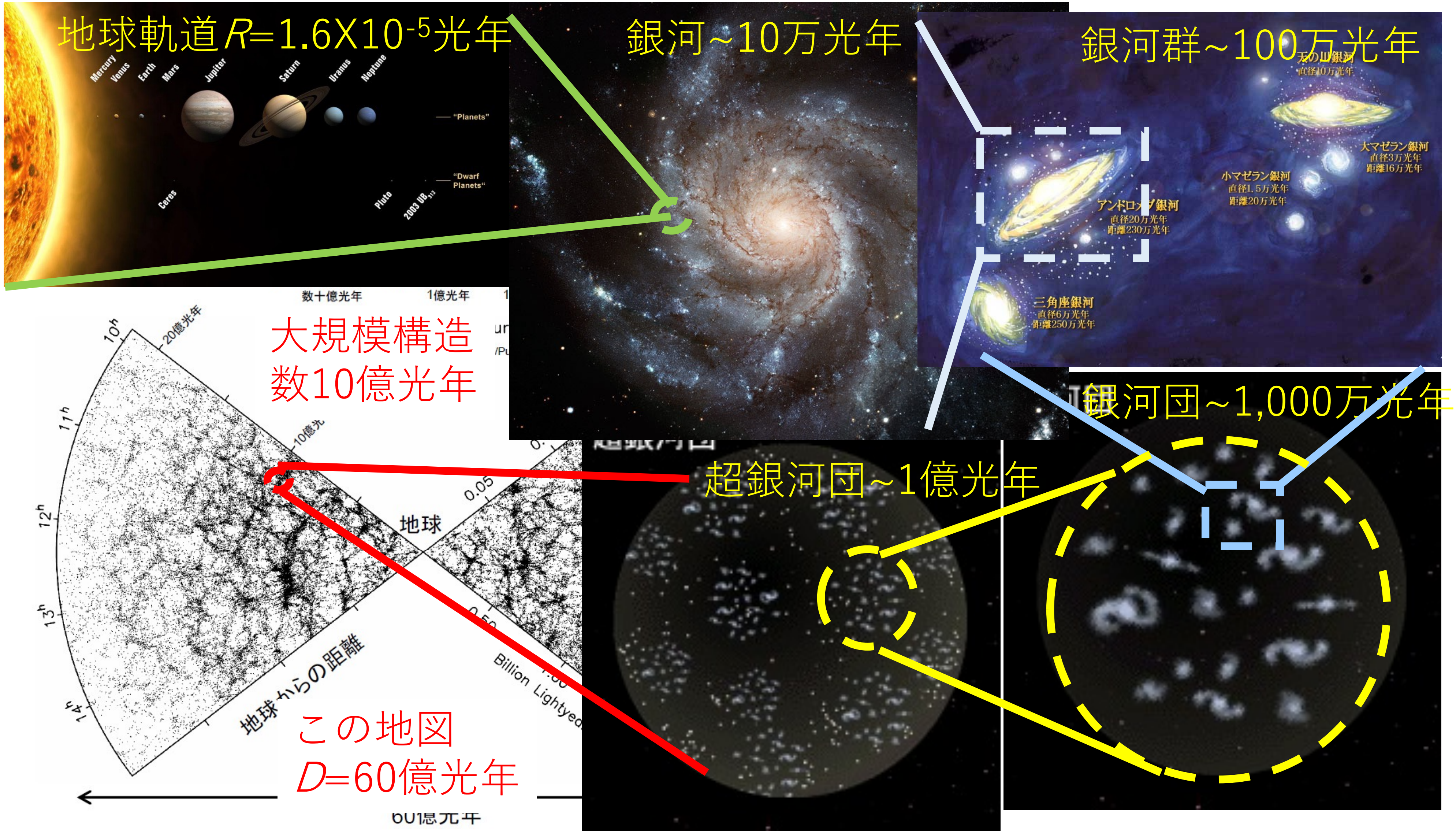
地球軌道R=1.6X10-5光年
銀河~10万光年
銀河群~100万光年
銀河団~1,000万光年
超銀河団~1億光年
大規模構造
数10億光年
この地図
D=60億光年
地球
地球からの距離
Mercury
Venus
Earth
Mars
Jupiter
Saturn
Uranus
Neptune
"Planets"
"Dwarf Planets"
Ceres
Pluto
天の川銀河
大マゼラン銀河
小マゼラン銀河
アンドロメダ銀河
三角座銀河
数十億光年
1億光年
20億光年
10億光
Billion Lightyea

Cosmic microwave background

- The Universe has been cooled down from the Big Bang.
  - $4x10^5$ y … Electron and proton coupled to H.
    - Light can freely go through in the Universe.

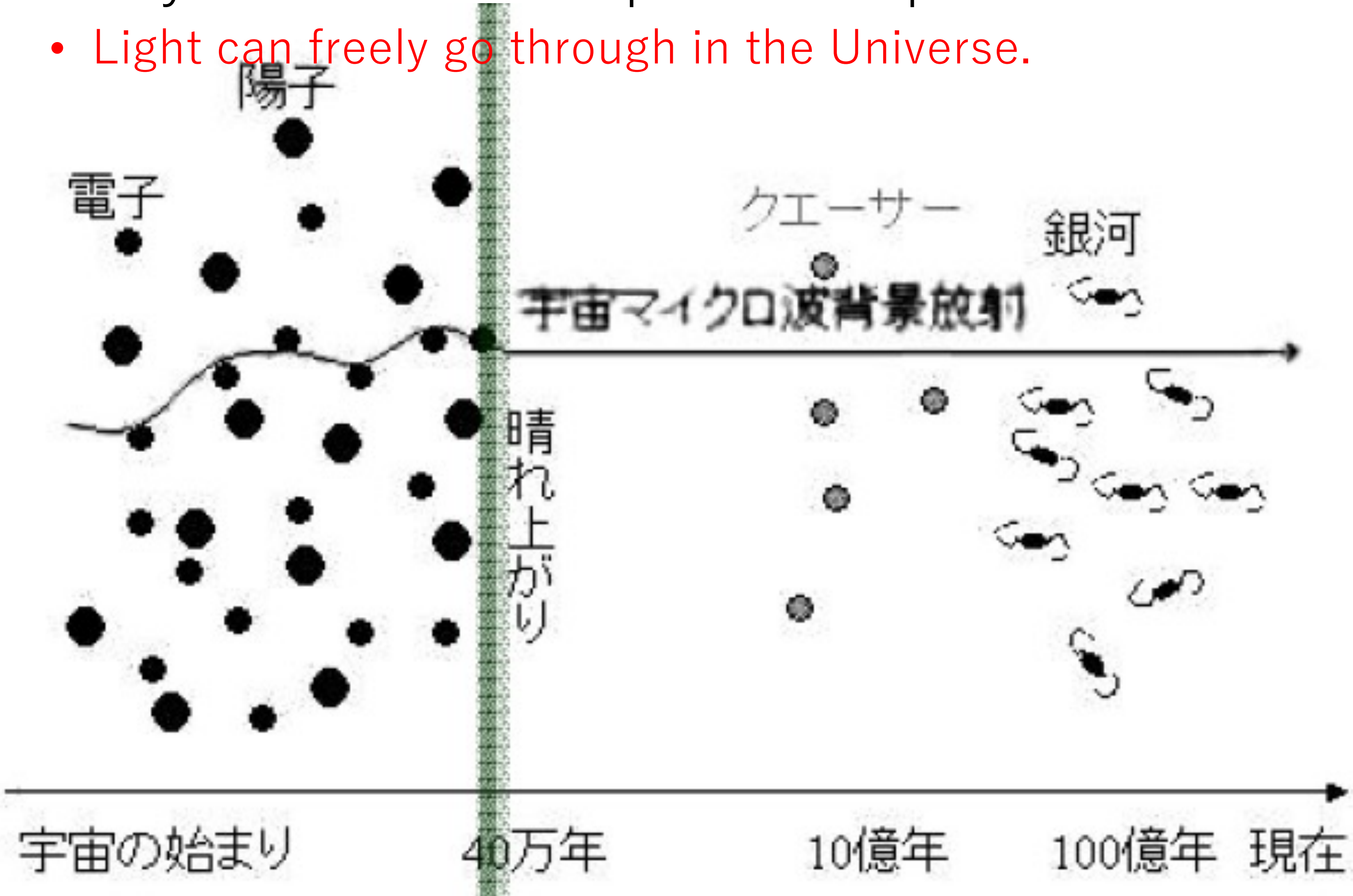

CMB measurement

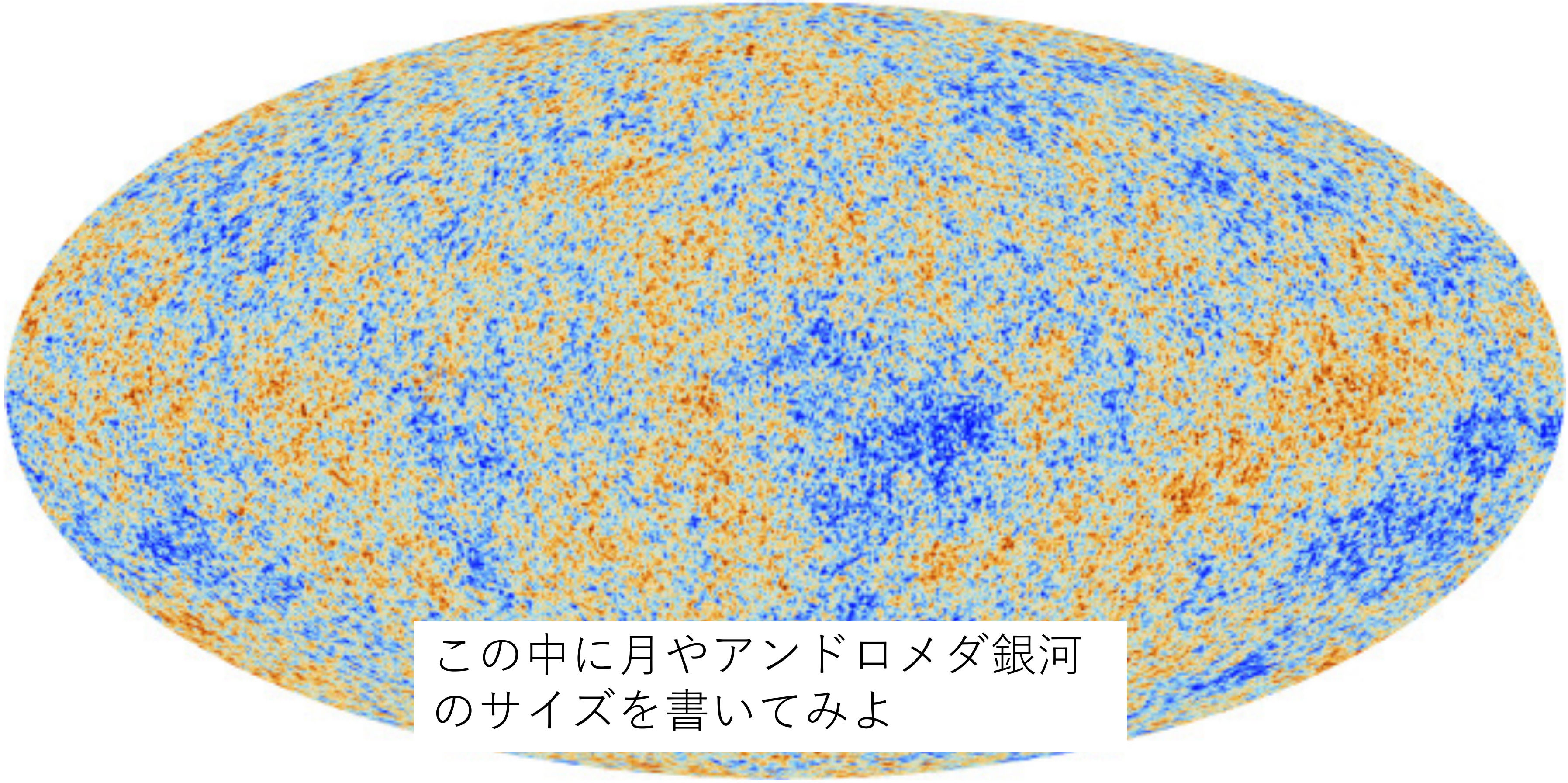

この中に月やアンドロメダ銀河
のサイズを書いてみよ

CMB results and DM

- Odd number peaks related to Ω_b
- Even number peaks related to Ω_m

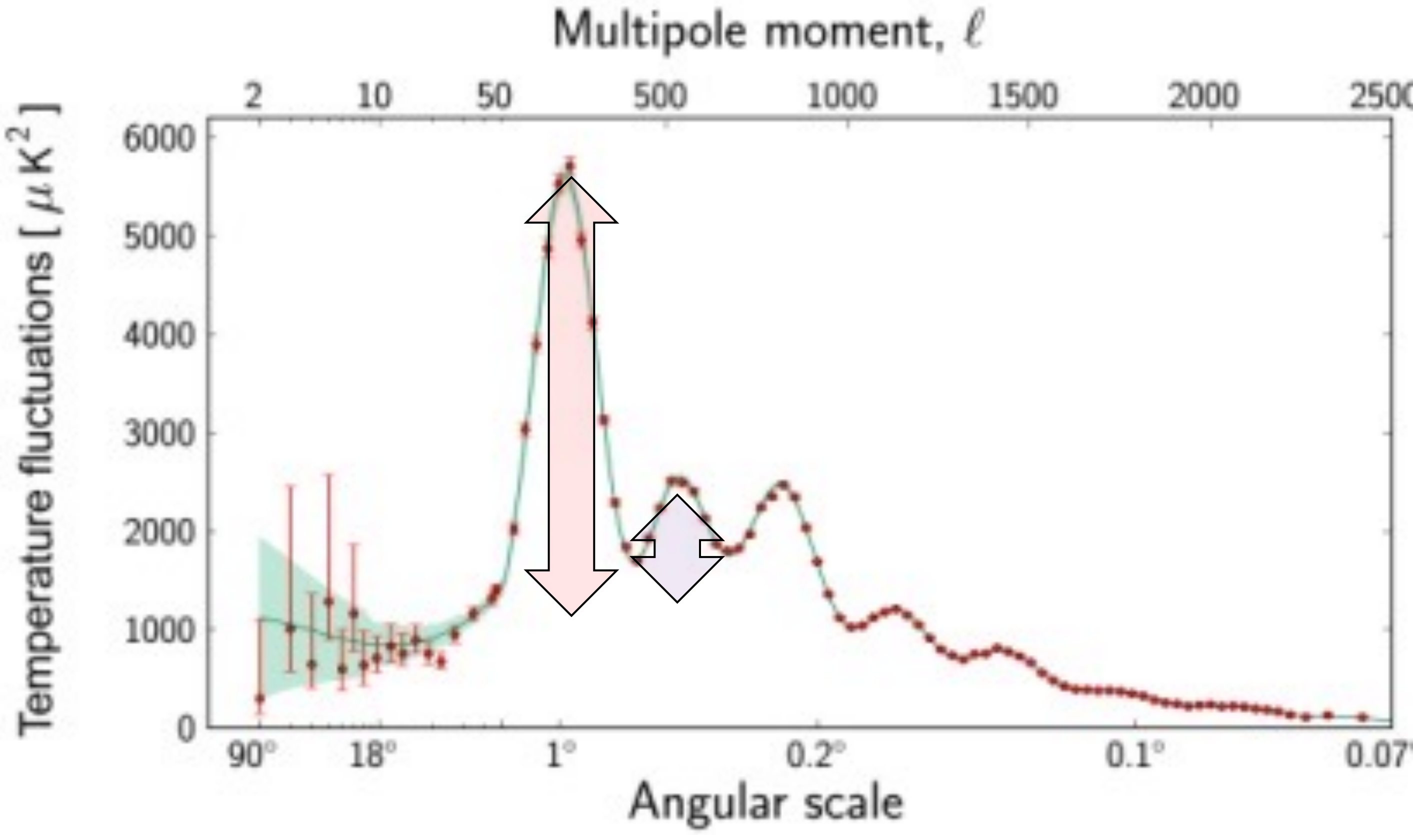

CMB results and DM

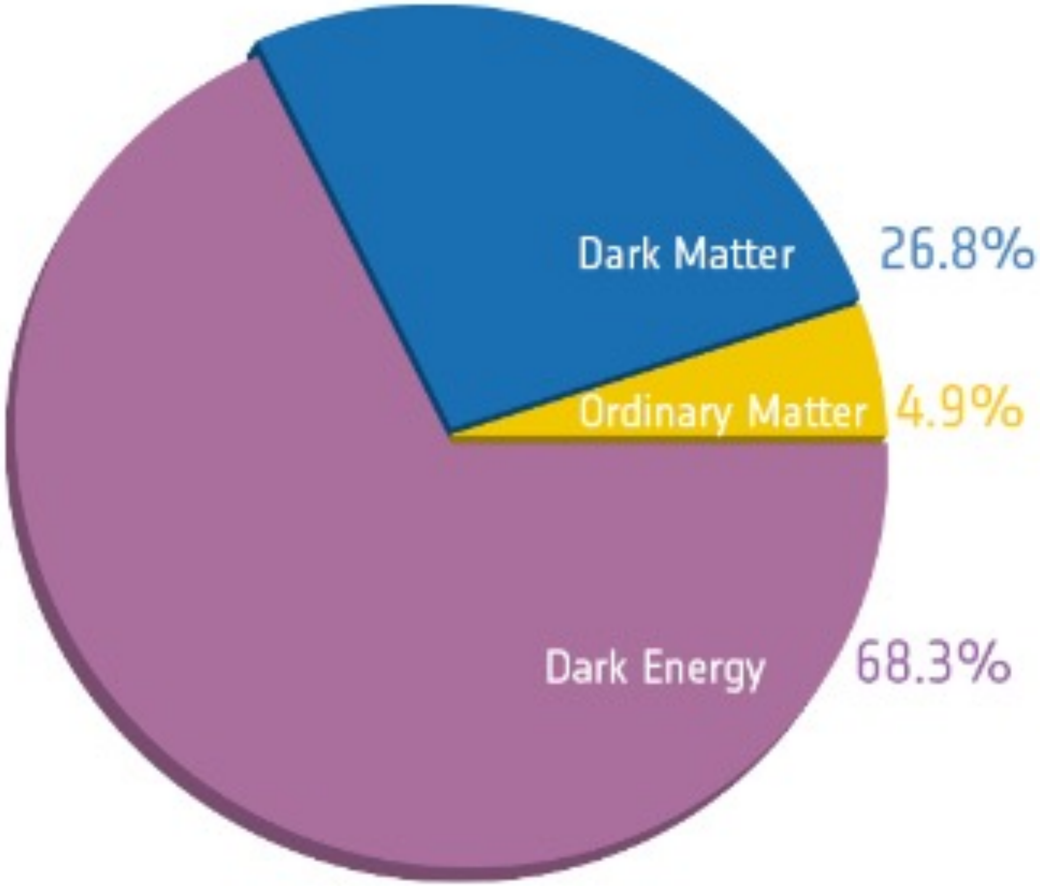

Galaxy cluster

- In the galaxy clusters scale, hot gas plays an important role.

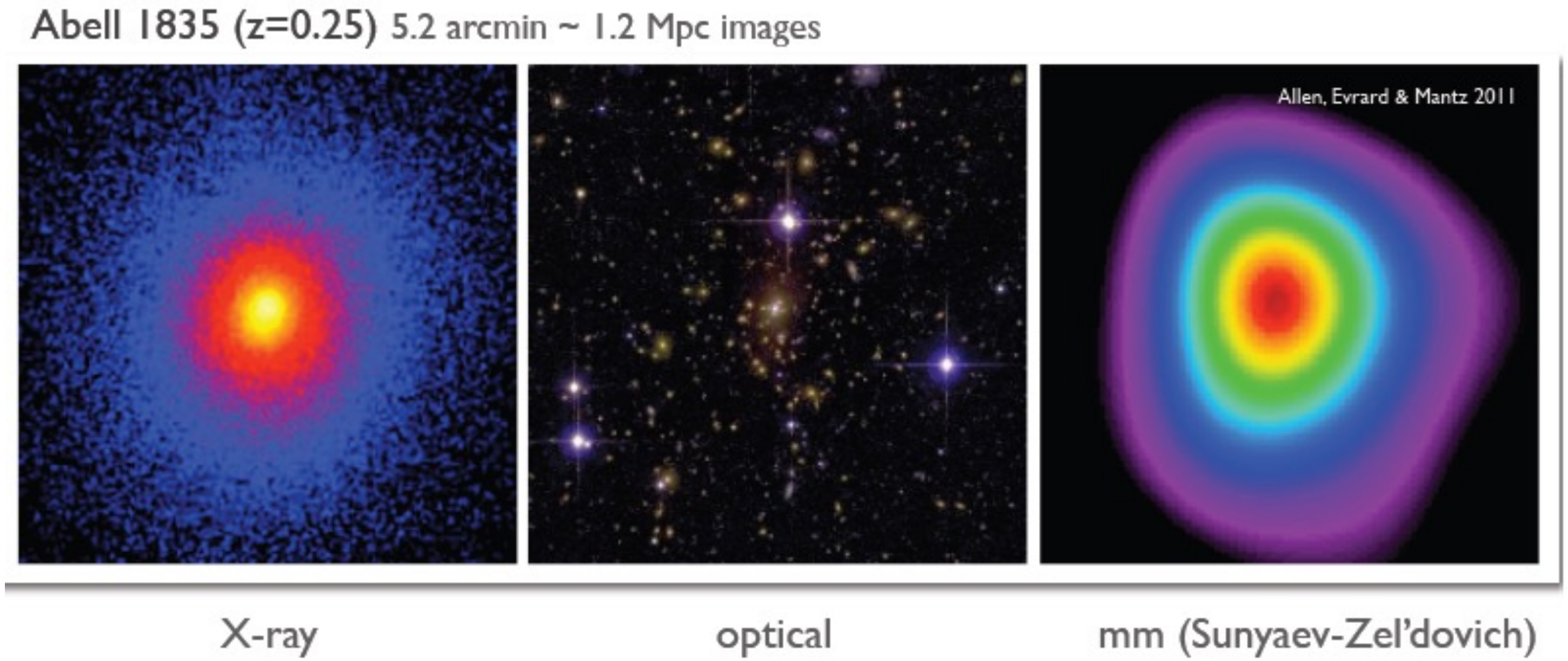

- Observation of high-temperature gas motion (T~8x10^{7}K)
- **M_{DM}/L~8-30**

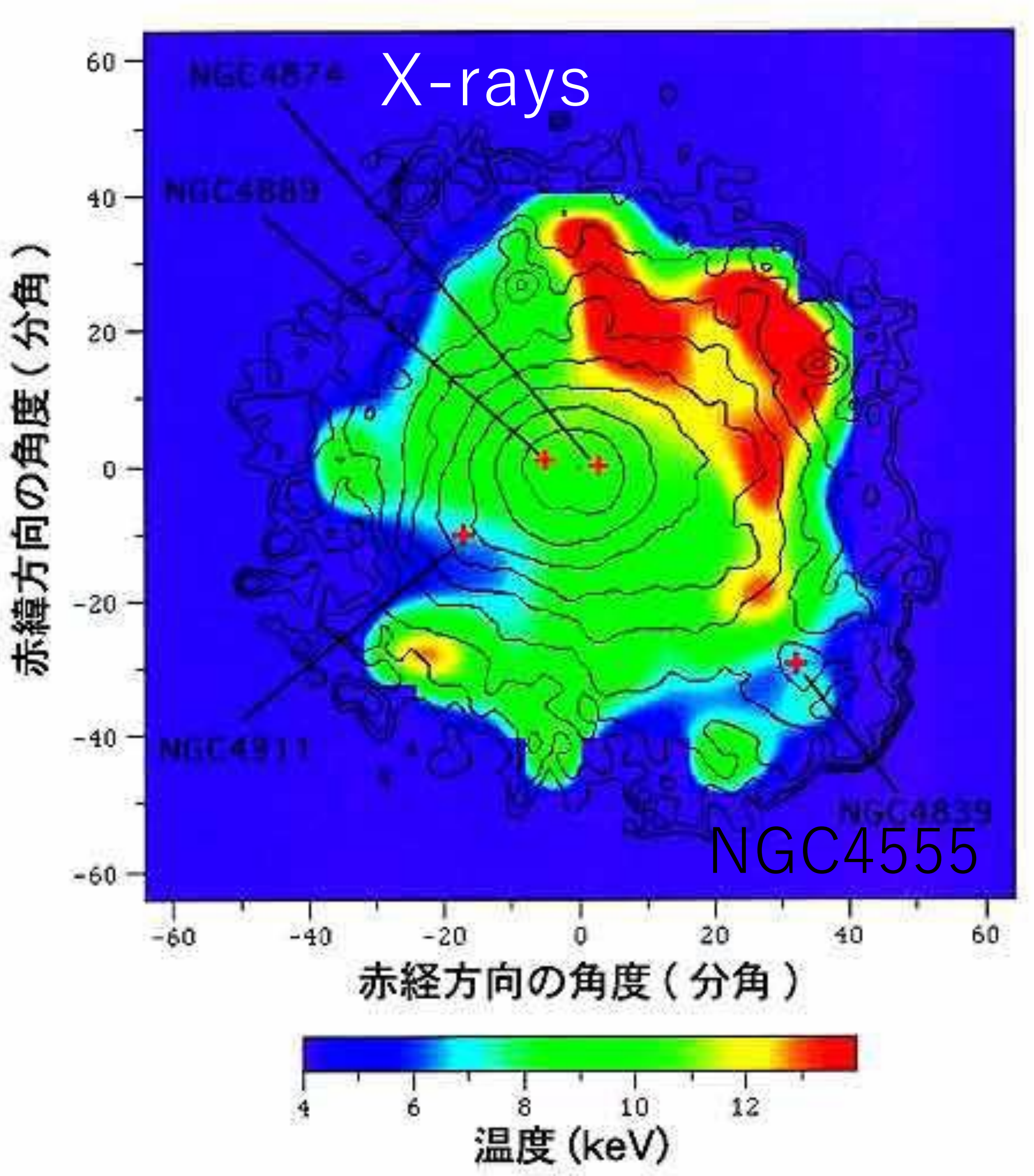

Elliptic galaxy

- X-ray observation of gas
- DM needs to attract the gas
  - $M_{\mathrm{DM}}/L \sim 10$

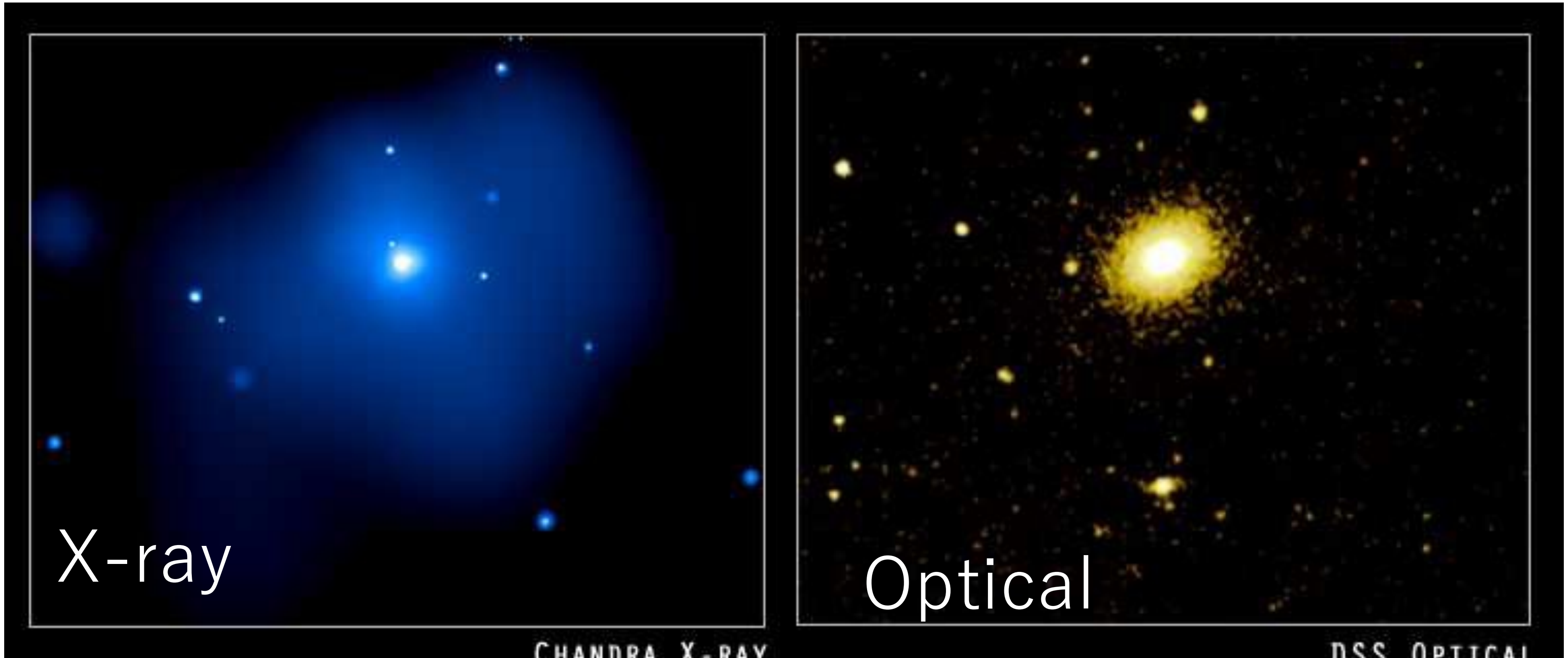

Spiral galaxy

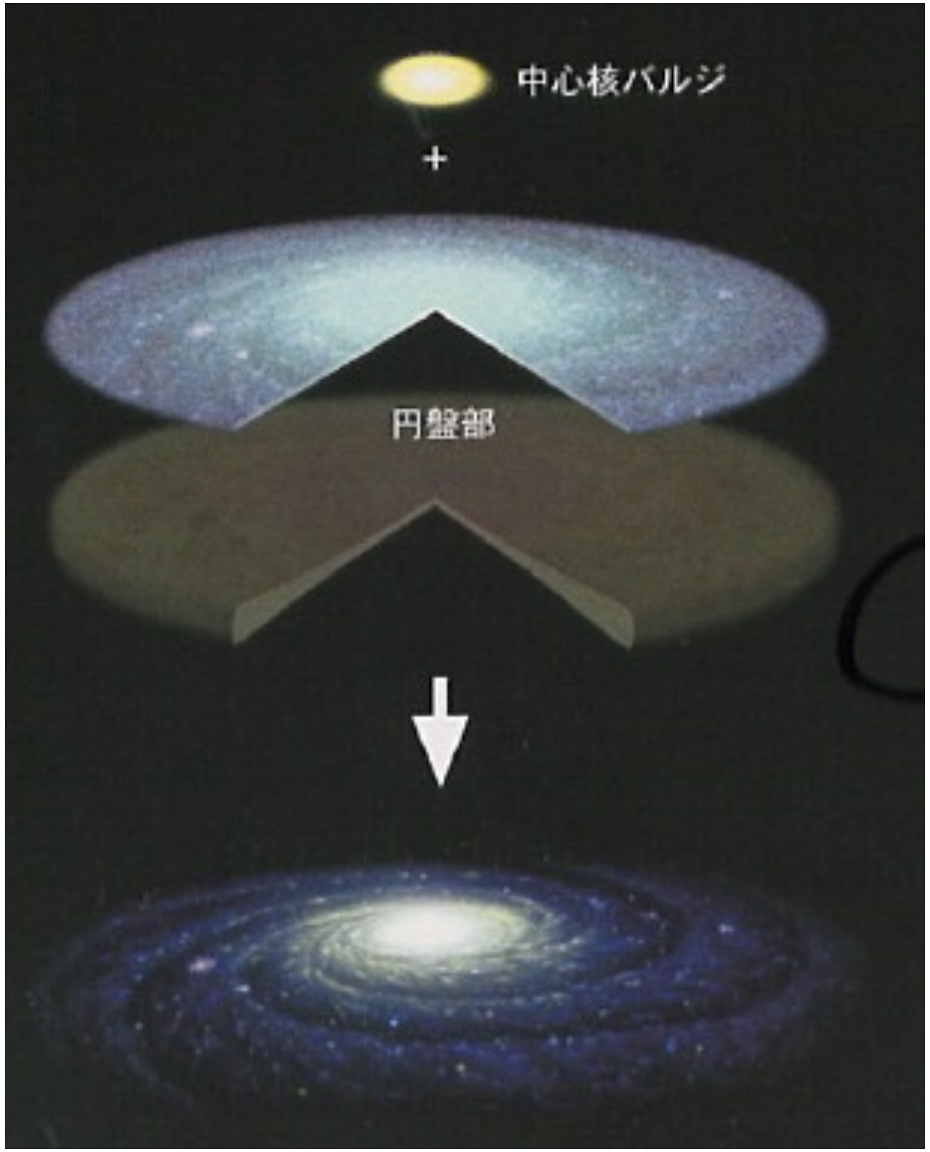

参考文献　「宇宙」沼澤茂美、脇屋奈々代
成美堂出版

Scale	DM	Note
The Solar sys.	No evidence yet.	
● Spiral galaxy ● Ellipse galaxy	● Rotational curve ● Kinematics of hot gas	● DM~x10 ● DM~x10
Cluster	● Kinematics of hot gas ● Kinematics of galaxies motion ● Micro-lensing	● DM~x8-30 ● DM~x3-4
Cosmological scale	● CMB ● Type Ia SNe ● BAO	● DM~x5 (*) ● DM~x6-7
Indication of DM	● Numerical studies on the structure formation	● Cold DM is favored. ● Hot DM is strongly disfavored. ● Warm DM ?

(*) There were(are?) also issues: not all of baryon in the Universe is observed. Missing Baryon.
But hot-gas amount in intra-cluster(ICM) media lead to large portion of baryon is in ICM.

- We cannot help convincing the presence of DM.

In our Galaxy

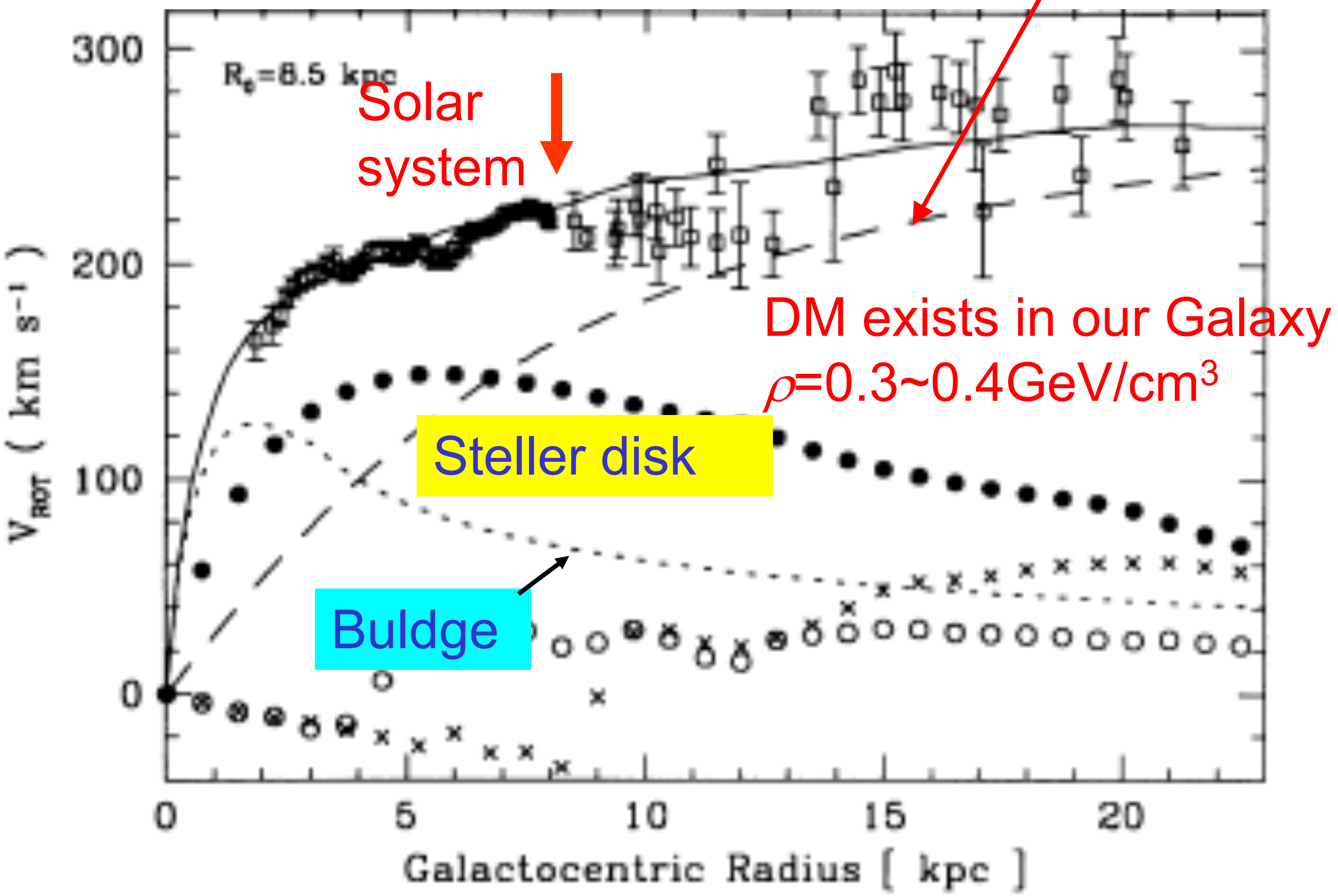

DM around us

- $\rho_{DM}^{\mathrm{local}} = (0.39 \pm 0.03)\,\frac{\mathbf{GeV}}{\mathbf{cm^3}}$
    - Value in PDB2014.
        - Fitting in 7- or 8 dim. parameters and galactic models.
    - This value is usually taken as a standard value.

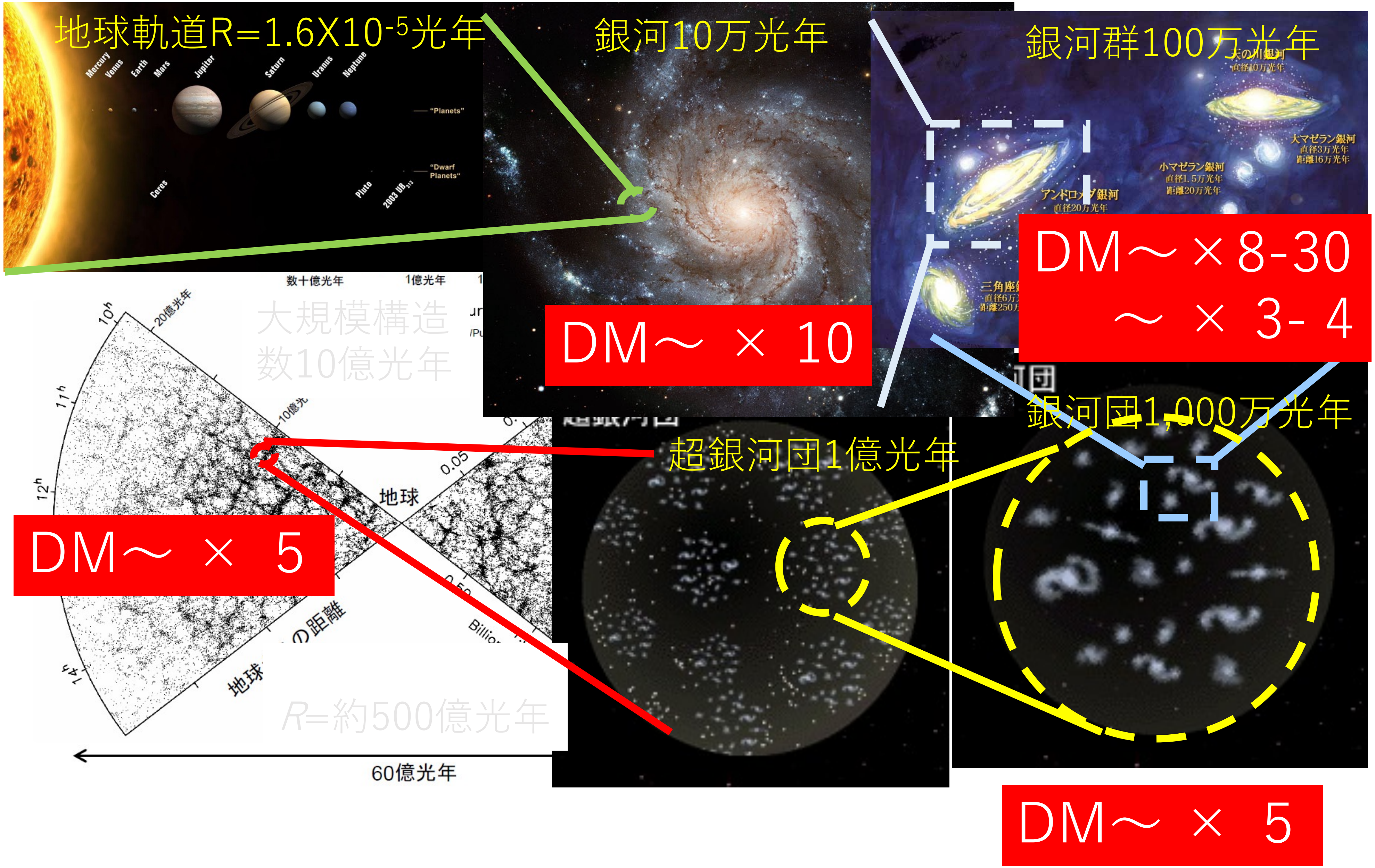
地球軌道R=1.6X10-5光年
Mercury
Venus
Earth
Mars
Jupiter
Saturn
Uranus
Neptune
"Planets"
"Dwarf Planets"
Ceres
Pluto
銀河10万光年
銀河群100万光年
天の川銀河
直径10万光年
大マゼラン銀河
直径3万光年
距離16万光年
小マゼラン銀河
直径1.5万光年
距離20万光年
直径20万光年
DM～×8-30
～ × 3- 4
DM～ × 10
銀河団1,000万光年
超銀河団1億光年
数十億光年
1億光年
大規模構造
数10億光年
20億光年
10億光
地球
0.05
の距離
地球
DM～ × 5
R=約500億光年
60億光年
DM～ × 5

- ここからAxionのはなし.
  - アクシオンは
    - θ 真空,
    - アノマリー
    - 強いCP問題
  - という３つのキーワードを解くカギを提供している.

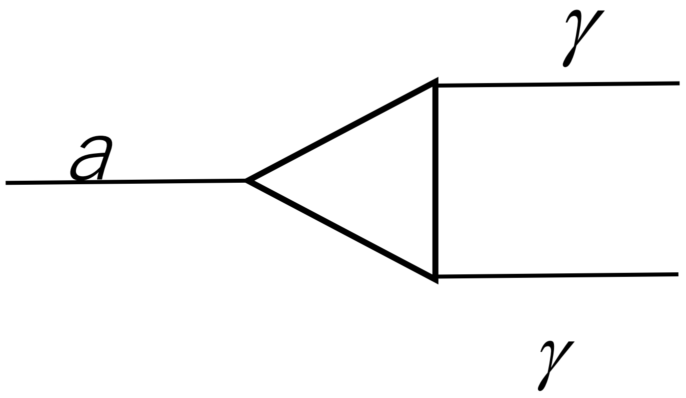

- Peccei-Quin 対称性
  - Standard Model の SU(3)×SU(2)×U(1) 対称性に加え，大局的なU(1)対称性（PQ対称性）を加える
  - （弱い対称性の破れに伴い，）PQ対称性も破れる．
    - この対称性の破れにともなう粒子として，アクシオンが現れる．
      - PQの議論では，2つ以上のHiggs 2 重項が必要で，中性Hi g g s の中にアクシオンの自由度が存在する
        - $\phi_1 = \frac{1}{\sqrt{2}} v_1 \exp\left(\frac{ia}{xv}\right), \phi_2 = \frac{1}{\sqrt{2}} v_2 \exp\left(\frac{ia}{v}\right), v = \sqrt{v_1^2 + v_2^2}, x = v_1/v_2$，a がアクシオン場
        - $m_a^2 = \frac{m_\pi^2 f_\pi^2}{v_{PQ}^2} \frac{m_u m_d}{(m_u+m_d)^2} \left(x + \frac{1}{x}\right)$

- 計算すると, $\frac{\theta}{16\pi} g_s^2 \mathrm{Tr}\, G_{\mu\nu}\tilde{G}_{\mu\nu}$ の部分で
  $\theta \rightarrow \theta + \frac{a}{v}\left(x + \frac{1}{x}\right)$ とすることができる.
  アクシオン場によって，CP対称性を破る部分を0にできる.
  「axion 場 a が， 最も低いポテンシャル位置に来ると，丁度， $\theta + \frac{a}{v}\left(x + \frac{1}{x}\right) = 0$ になる」

- ところで， この一連の議論の中で,
  アクシオン質量は以下の様に１つに決まる.
  - $m_a^2 = \frac{m_\pi^2 f_\pi^2}{v_{PQ}^2} \frac{m_u m_d}{(m_u + m_d)^2} \left(x + \frac{1}{x}\right)$
  - $\theta + \frac{a}{v}\left(x + \frac{1}{x}\right) = 0$ を選ぶ代わりに，アクシオン質量は，強い相互作用の性質に強く関連付けられる結果となる

アクシオンいろいろ

- （オリジナルの）アクシオン(standard axion)
  - 弱い相互作用における対称性の破れ＝PQ対称性の破れ
    - $v_{EW} = \left(\sqrt{2}G_F\right)^{-1} = 247\ \mathrm{GeV} = v_{PQ}$
  - $m_a \sim 73\left(x + \frac{1}{x}\right)$ keV となり，実験と矛盾

- Invisible axion
  - PQ対称性の破れが，EWの対称性の破れよりも，高いエネルギー領域で起こったと考える．
    - $v_{PQ} \to f_A$
  - 結果，もっと軽いアクシオンが強いCP問題を解決する

    - この辺り，詳細に興味があれば，長嶋先生の朝倉のを参照

シリーズ現代の天文学２「宇宙論１」から

DM axion

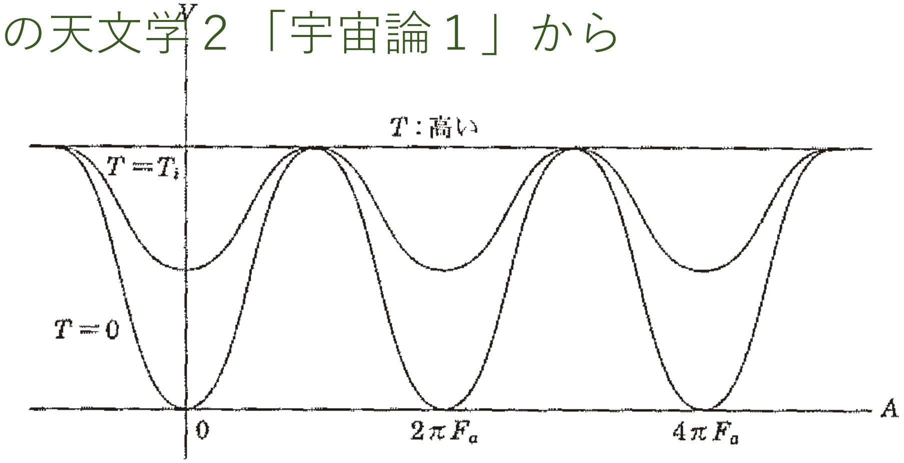

図 5.14　アクシオン場のポテンシャル.

- Axion mass and breaking scale:
  - $m_a \sim 6.2\times10^{-4}\ eV\left(\frac{10^{10}\mathrm{GeV}}{f_a}\right)$
- Axion is supposed to be produced by **miss-alignment mechanism**.
  - → It is *not* thermally produced.
  - Axion is categorized as *cold* DM though it has light mass.

- Current axion density:
  - $\Omega_a h^2 \sim 0.16 \left(\frac{m_a}{10^{-5} e\mathrm{V}}\right)^{-1.18} \bar{\theta}_i^2,$
    - where $\overline{\theta_i}$ is mean of initial θ at the symmetry breaking.

  - m_a が小さいと 宇宙をOver close
  - m_a が大きいとＤＭに足りなくなる
    - 境界が 10μeV 位

- 参考文献：シリーズ現代の天文学２「宇宙論１」

- しかし，宇宙の位相欠陥からＡｘｉｏｎが無視しえない量発生するので，質量上限が上がった.

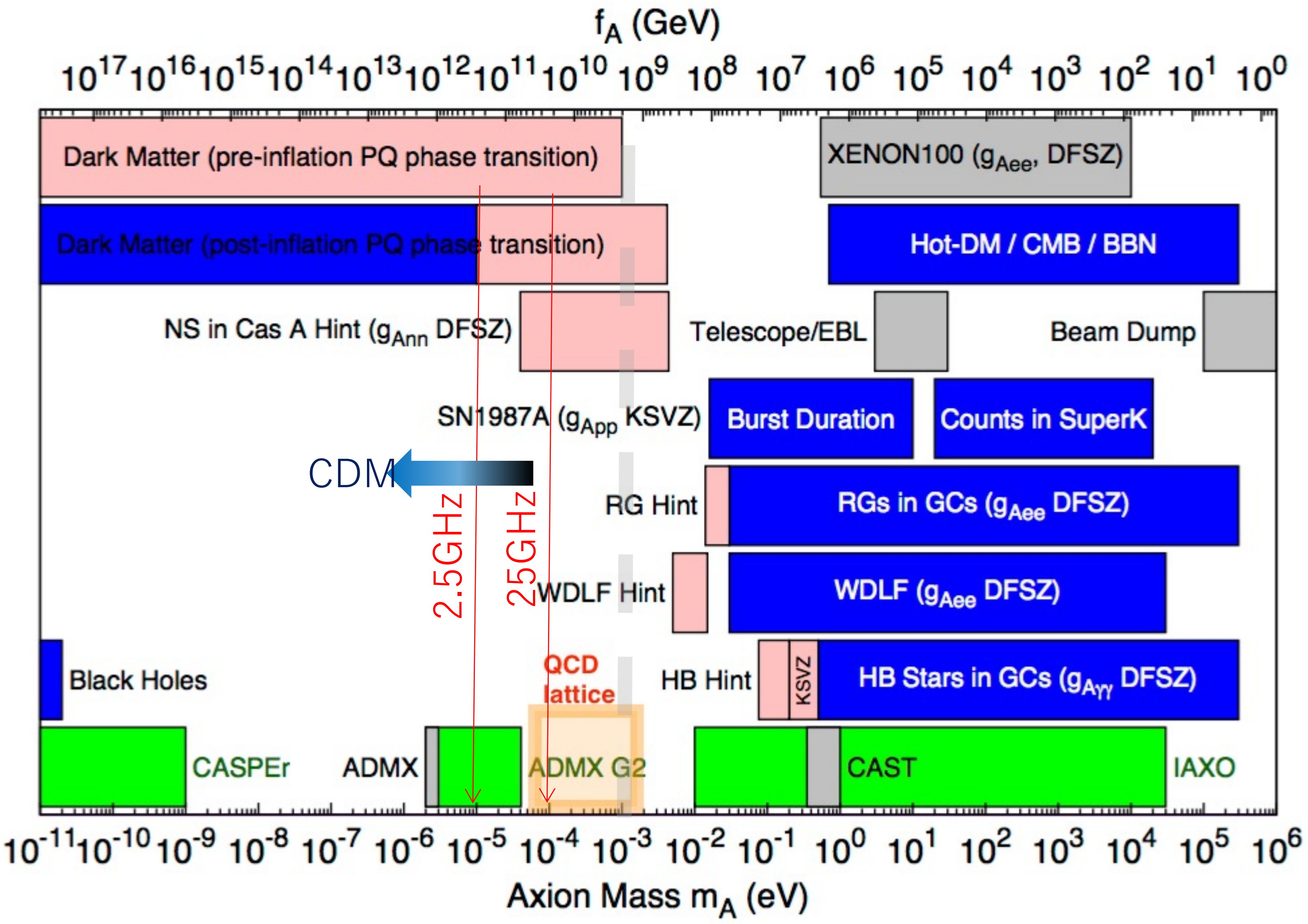

f_A (GeV)
10^{17} 10^{16} 10^{15} 10^{14} 10^{13} 10^{12} 10^{11} 10^{10} 10^{9} 10^{8} 10^{7} 10^{6} 10^{5} 10^{4} 10^{3} 10^{2} 10^{1} 10^{0}
Dark Matter (pre-inflation PQ phase transition)
XENON100 (g_{Aee}, DFSZ)
Dark Matter (post-inflation PQ phase transition)
Hot-DM / CMB / BBN
NS in Cas A Hint (g_{Ann} DFSZ)
Telescope/EBL
Beam Dump
SN1987A (g_{App} KSVZ)
Burst Duration
Counts in SuperK
CDM
RG Hint
RGs in GCs (g_{Aee} DFSZ)
2.5GHz
25GHz
WDLF Hint
WDLF (g_{Aee} DFSZ)
QCD lattice
Black Holes
HB Hint
KSVZ
HB Stars in GCs ($g_{A\gamma\gamma}$ DFSZ)
CASPEr
ADMX
ADMX G2
CAST
IAXO
10^{-11} 10^{-10} 10^{-9} 10^{-8} 10^{-7} 10^{-6} 10^{-5} 10^{-4} 10^{-3} 10^{-2} 10^{-1} 10^{0} 10^{1} 10^{2} 10^{3} 10^{4} 10^{5} 10^{6}
Axion Mass m_A (eV)

Axion 探索のための相互作用

- $g_{a\gamma\gamma}$：
  - 「アクシオン」である限り，必ず存在する
    - これは，アノマリー項から来る（らしい）．
    - 実験的にはスカを食らいたくないので，この相互作用を使う事が好まれる．
- g_{aee}：
  - アクシオンは「強い相互作用」の申し子である
    レプトンには結合しないのが自然.
  - GUTの立場に立てば，レプトンとクオークを区別するのは不自然.
  - 結局，モデルに依る．
    - 実験的には，電子と相互作用してくれるなら，明らかに $a-e$ 結合を使うのが高感度の設計がやりやすいはず.

アクシオンの検出

- アクシオンは，ループダイアグラムを通じて，２つの光子と結合する．
    - このループの中で何を取るか？によってモデル依存性がある．
  - $\mathcal{L} = -G_a \boldsymbol{E} \cdot \boldsymbol{B} a$
- **外部から磁場**を印可して，
  - $a + \gamma(B) \to \gamma$

　の反応で出ている 光子を探索することが最も効率が良いとされている．

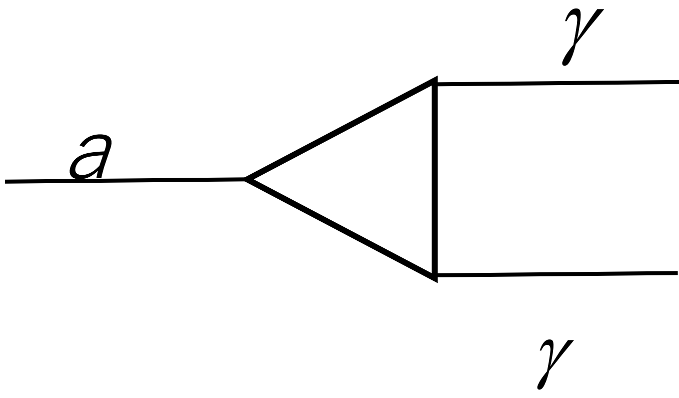

- 外部からの「電場」では？
  - 次の理由から磁場が好ましい
  - １）　用意できる磁場と電場を比較すると，磁場の方が強い
    - 宿題
      - 自然単位系で 1 T と 1 V/m を計算し，
      - 次に，磁場で用意できる ～10 T と放電限界の ～10^6 V/m を比べると良い
    - 例外は，結晶中の電場．これを上手く使うことができるか？
  - ２）　$\mathcal{L} = -g_{a\gamma\gamma}\boldsymbol{E}\cdot\boldsymbol{B}\,a$ の具体形をかくと，
    - $\mathcal{L} \propto E_{\mathrm{Ext.}} B_{\mathrm{signal}} \partial_x\, a$ → アクシオンの速度が速いときのみ
      - 太陽AxionにはOK（それでも，用意できる電場に限界あり）
      - DM Axionではダメ
    - Or $\mathcal{L} \propto E_{\mathrm{signal}}\, B_0 \partial_t^2 a$ → アクシオンの速度に無関係
      - 太陽Axion にはOK
      - DM Axion にもOK

実験的にアクシオンを探索する際のベンチマークモデル

- KSVZ アクシオンモデル
  - レプトンとアクシオンが相互作用しない
- DFSZ アクシオンモデル
  - レプトンとアクシオンは相互作用する

- ※ $g_{a\gamma\gamma}$ の場合，結合する粒子の種類が多く，しかも軽い電子が相互作用する，DFSZモデルの方が $g_{a\gamma\gamma}^2$ が大きいように想像する．
- しかし，実際は逆で，KSVZモデルの方が $g_{a\gamma\gamma}^2$ が大きい．

- g_{ae}を使う事も考えられるが，ハズレるとかなり悲しい
  - そのため， 実験的な探索では $g_{a\gamma\gamma}$ が主役となっている

「用語」の整理

- QCD アクシオン
  - 強い相互作用におけるCP問題を解決するためのAxionモデル
  - 質量と結合定数に相関がある.
    - KSVZ とか，DFSZとかはこれに相当する.
    - QCD Axion のうちで，一番制限を緩くできないかを追求した１つの例が，暗黒物質Axionモデルの「Trapped misalignment model」
- Axion-like particle (ALP), アクシオン様粒子
  - QCDなんか忘れてしまったもの.
    - その代わり，超弦理論とかが起源．由緒ある粒子.
  - 質量と結合定数との相関に制限がない，ゆるい
    - 1つの例が，物理教室 高橋先生のALP miracle

- 太陽アクシオン
  - 太陽中で作られ，放出されている
- 暗黒物質アクシオン
  - 暗黒物質として，存在しているアクシオン
- その他，超新星アクシオンとか，存在形態が名前になっているもの

- ※ アクシオンは，QCDの要請に由来するので，多分存在する.
- 存在するならば，ほぼ間違い無く，太陽から放出されている.
    - 太陽の温度 > Axion質量のとき
- 論理的には，アクシオンが存在しても，暗黒物質である必然性はない.
- しかし，暗黒物質になり得る質量領域では，太陽アクシオンを探索する事は，結合定数が小さすぎて不可能.
- 結局，<u>太陽アクシオンと暗黒物質アクシオンの両方から攻めるしかない</u>.

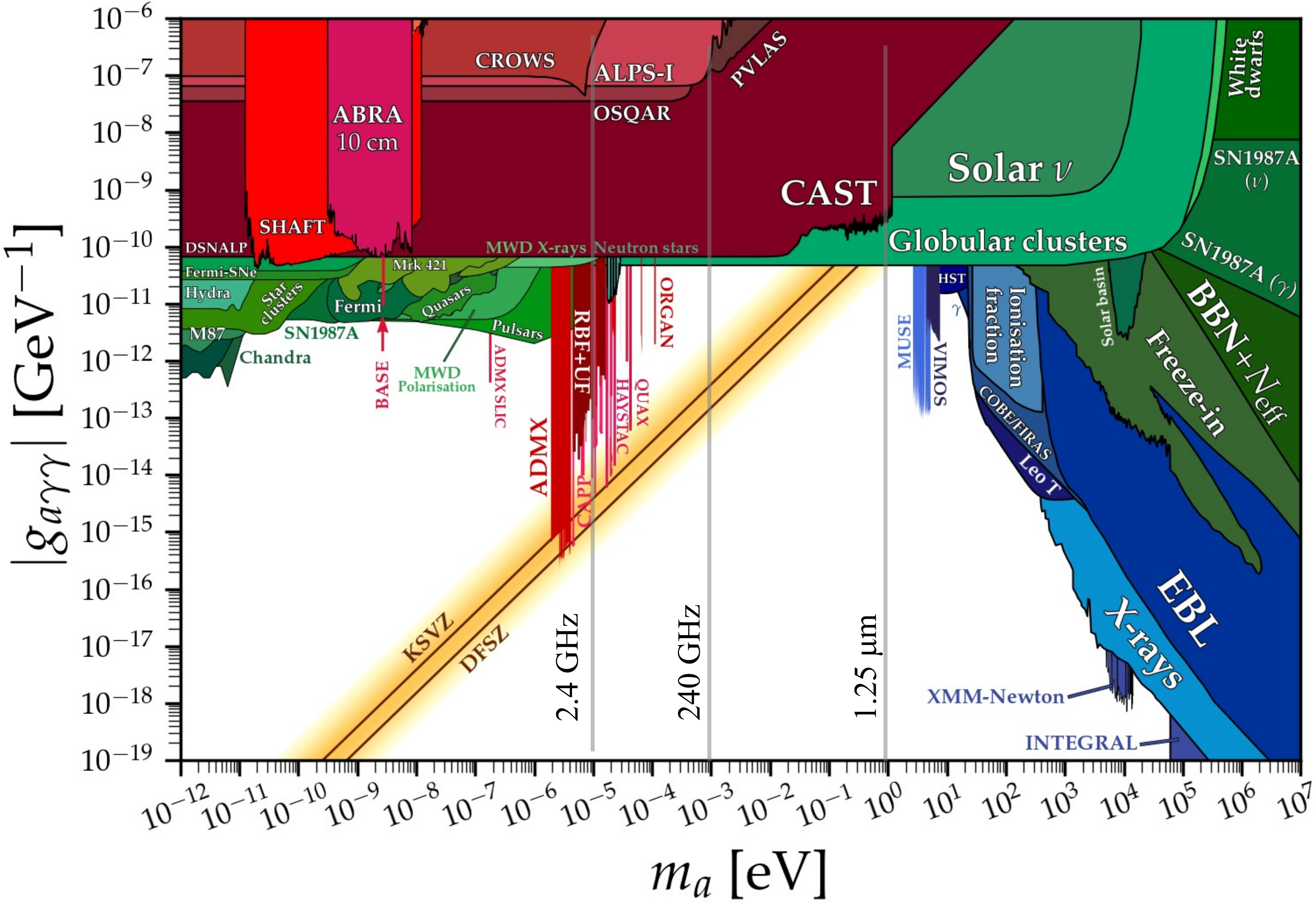

https://cajohare.github.io/AxionLimits/docs/ap.html

Axion production in the Sun

- Atomic recombination
- Bremsstrahlung
- Compton scattering
- Primakov conversion
- X-ray emission from M1 transition
  - ^{57}Fe

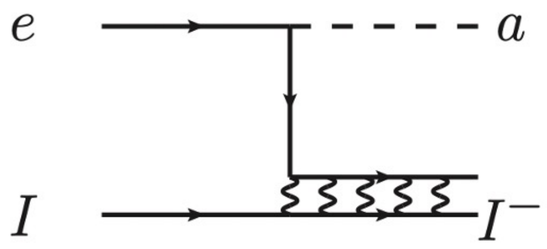

axiorecombination

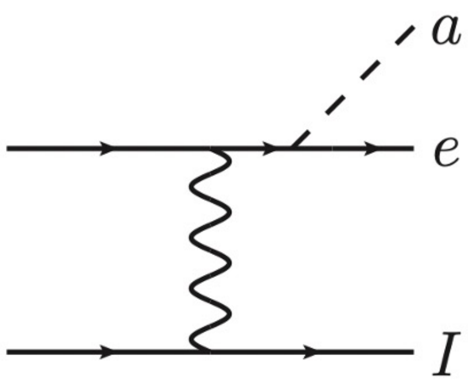

e − I bremsstrahlung

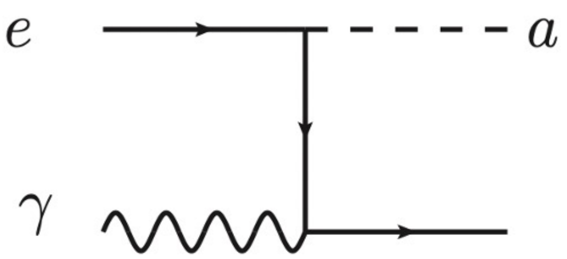

Compton

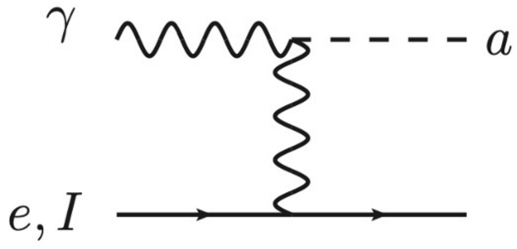

Primakoff

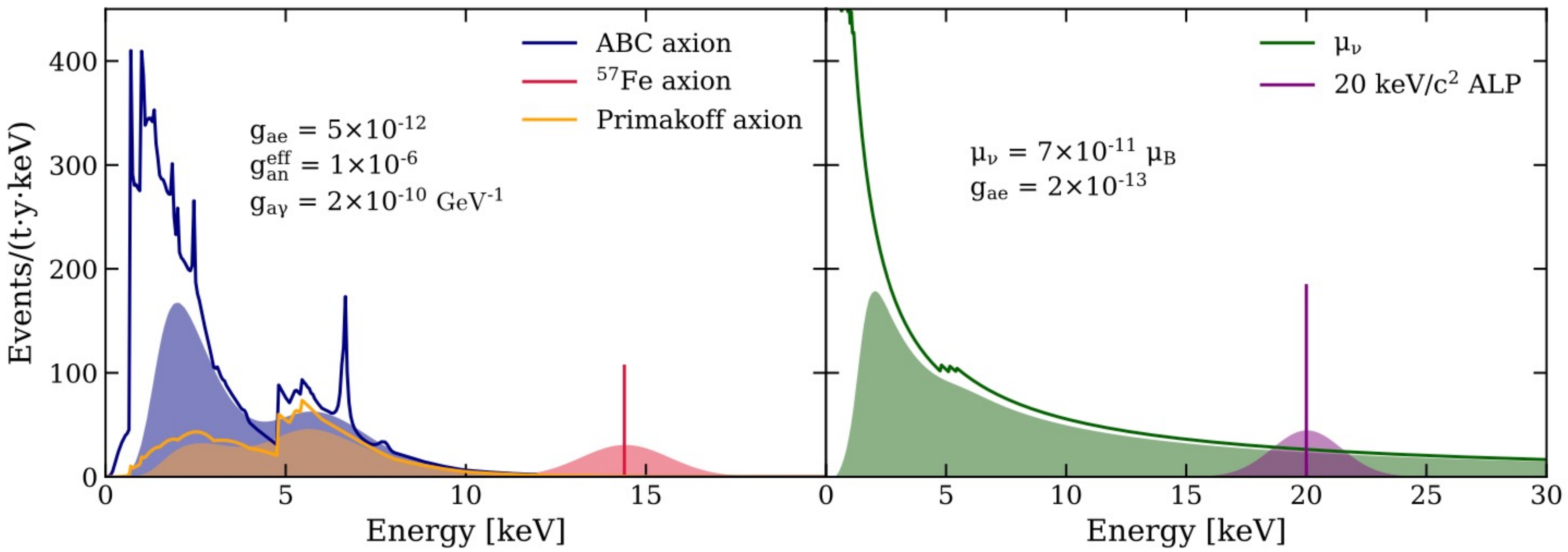

FIG. 1. Left: Expected signal in energy space for ABC solar axions with a coupling $g_{ae} = 5 \times 10^{-12}$ (blue), for solar axions produced from the de-excitation of ^{57}Fe with coupling $g_{an}^{eff} = 1 \times 10^{-6}$ (red), and for solar axions produced from the Primakoff effect with coupling $g_{a\gamma} = 2 \times 10^{-10}$ (orange). Right: Signature of an enhanced neutrino magnetic moment with magnitude $7 \times 10^{-11}\, \mu_B$ (green) and a 20 keV/c^2 ALP with coupling constant $g_{ae} = 2 \times 10^{-13}$ (purple). Both the true deposited energy spectra in a xenon detector without efficiency loss (unshaded) and the expected observed spectra in XENON1T including the specific detector resolution and efficiency (shaded) are shown.

Axion Helioscope
(Sikivie 1983)

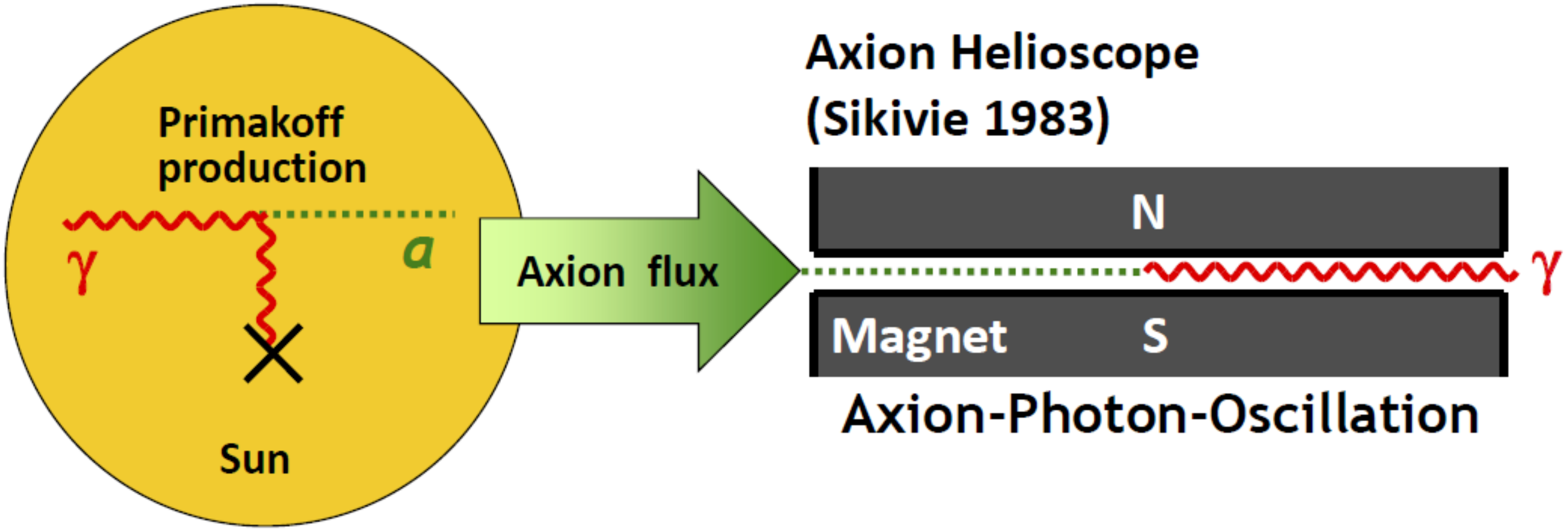

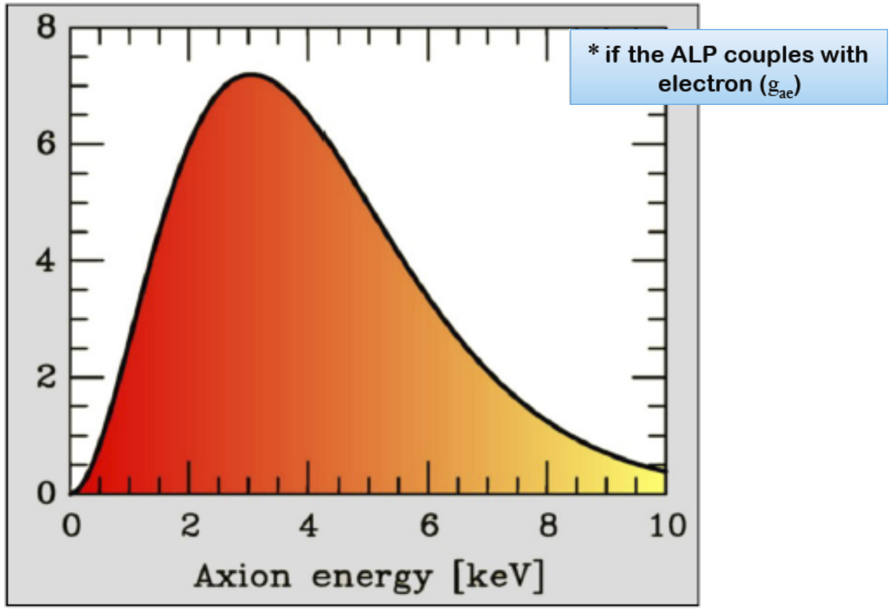

- Tokyo Axion Helioscope (“Sumico”)
(Results since 1998, up again 2008)
- CERN Axion Solar Telescope (CAST)
(Data since 2003)

Alternative technique:
Bragg conversion in crystal
Experimental limits on solar axion flux from dark-matter experiments (SOLAX, COSME, DAMA, CDMS ...)

Solar axion detection

PHYSICAL REVIEW D
PARTICLES AND FIELDS

THIRD SERIES, VOLUME 39, NUMBER 8 15 APRIL 1989

Design for a practical laboratory detector for solar axions

K. van Bibber
Physics Department, Lawrence Livermore National Laboratory, University of California, Livermore, California 94550

P. M. McIntyre
Physics Department, Texas A&M University, College Station, Texas 77843

D. E. Morris
Physics Division, Lawrence Berkeley Laboratory, University of California, Berkeley, California 94720

G. G. Raffelt
*Institute for Geophysics and Planetary Physics, Lawrence Livermore National Laboratory, University of California, Livermore, California 94550
and Astronomy Department, University of California, Berkeley, California 94720*

(Received 19 September 1988)

We present a practical design for a detector sensitive to axions and other light particles with a two-photon interaction vertex. Such particles would be produced in the solar interior by Primakoff conversion of blackbody photons and could be detected by their reconversion into x rays (average energy about 4 keV) in a strong laboratory magnetic field. An existing large superconducting magnet would be suitable for this purpose. The transition rate is enhanced by filling the conversion region with a buffer gas (H_2 or He). This induces an effective photon mass (plasma frequency) which can be adjusted to equal the axion mass being searched for. Axion-photon conversion is then coherent throughout the detector volume for all axion energies. Axions with mass in the range 0.1 eV $\lesssim m_a \lesssim$ 5 eV can be detected using gas pressures of 0.1–300 atm. Axions with the standard coupling strength to photons would give counting rates of 10^{-5}–$10 \sec^{-1}$ over this mass range. The search would definitively test one of the only two regions of axion parameters not excluded by astrophysical constraints.

Solar axion detection

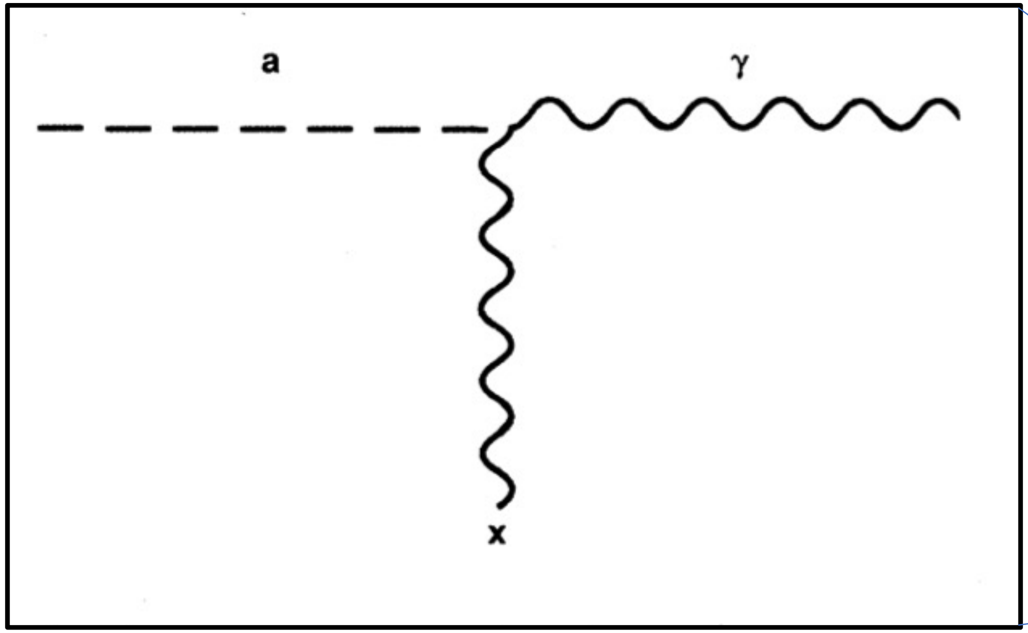

吸収が無視できる場合,

$$p_\gamma \to \left(\frac{BL}{2M}\right)^2 \frac{\sin^2 qL}{(qL)^2}, \quad q \equiv \frac{m_\gamma^2 - m_a^2}{2E_\gamma}$$

THIRD SERIES, VOLUME 39, NUMBER 8 15 APRIL 1989

Design for a practical laboratory detector for solar axions

K. van Bibber
Physics Department, Lawrence Livermore National Laboratory, University of California, Livermore, California 94550

P. M. McIntyre
Physics Department, Texas A&M University, College Station, Texas 77843

D. E. Morris
Physics Division, Lawrence Berkeley Laboratory, University of California, Berkeley, California 94720

G. G. Raffelt
Institute for Geophysics and Planetary Physics, Lawrence Livermore National Laboratory, University of California, Livermore, California 94550
and Astronomy Department, University of California, Berkeley, California 94720
(Received 19 September 1988)

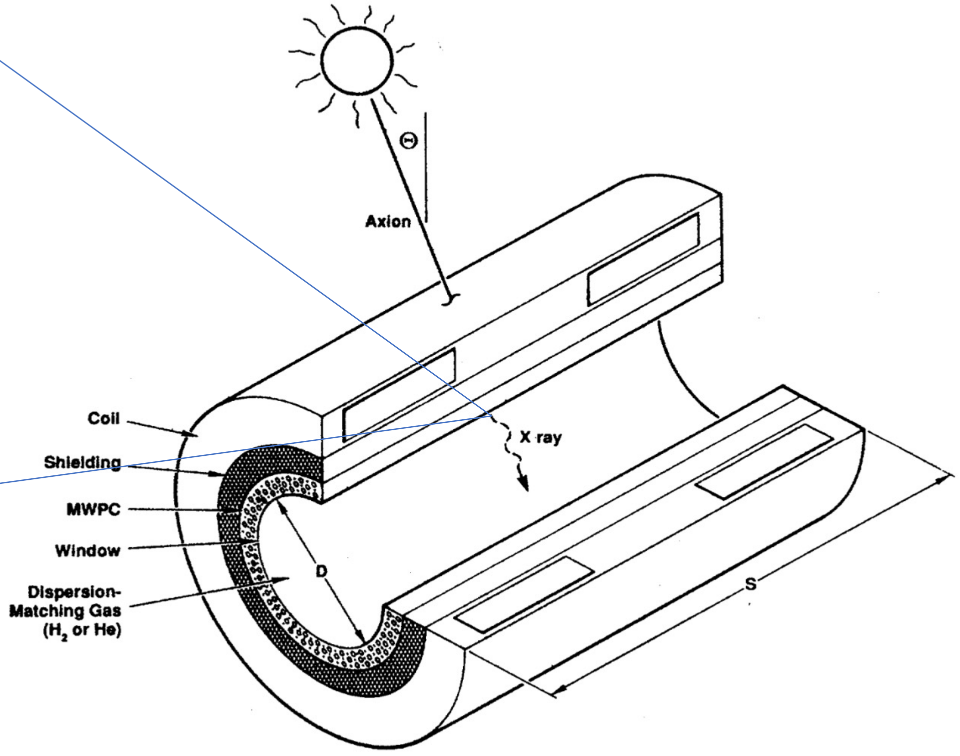

FIG. 4. Schematic design of the detector employing a multiple-wire proportional chamber (MWPC).

- 磁場中のAxionと光子の転換を波動論的に解く

$\langle A(z)|\, a(0)\rangle$ を解いて,
$p(z) = |\langle A(z)|a(0)\rangle|^2$ を計算

$$i\partial_z \begin{bmatrix} A \\ a \end{bmatrix} = \begin{bmatrix} \omega - m_\gamma^2/2\omega - i\Gamma/2 & B/2M \\ B/2M & \omega - m_a^2/2\omega \end{bmatrix} \begin{bmatrix} A \\ a \end{bmatrix} \quad (11)$$

$\Gamma = \frac{1}{L_{abs}}$, L_{abs} = Absorption length of signal X-rays

$$p_\gamma(L) = \frac{(B/2M)^2}{q^2+\Gamma^2/4}[1+e^{-\Gamma L} - 2e^{-\Gamma L/2}\cos(qL)] .$$

$$q = |(m_\gamma^2 - m_a^2)/2\omega|$$

ω = Signal X-ray energy
m_a = mass of photon in a detector
(Usually, zero. But some cases, non-zero.

In $\Gamma \to 0$, $p_\gamma \to \left(\frac{BL}{2M}\right)^2 \frac{\sin^2 qL}{(qL)^2}$

CAST

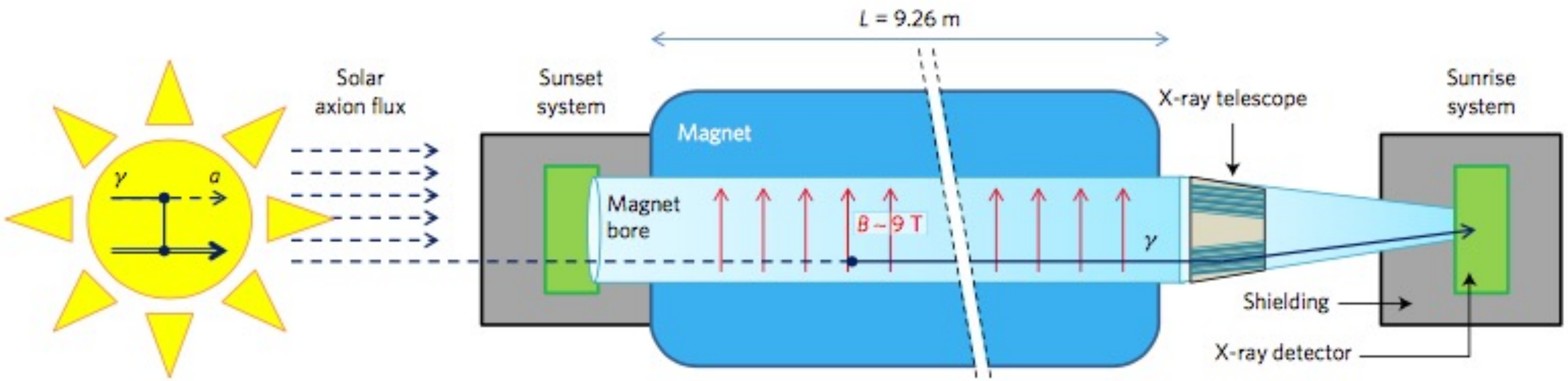

Figure 1 | Sketch of the CAST helioscope at CERN to search for solar axions. These hypothetical low-mass bosons are produced in the Sun by Primakoff scattering on charged particles and converted back to X-rays by the same process in the *B*-field of an LHC test magnet. The two straight conversion pipes have a cross-section of 14.5 cm^2 each. The magnet can move by ±8° vertically and ±40° horizontally, enough to follow the Sun for about 1.5 h at dawn and dusk with each end of the magnet, where separate detection systems can search for axions at sunrise and sunset, respectively. The sunrise system is equipped with an X-ray telescope (XRT) to focus the signal on a small detector area, strongly increasing signal to noise. Our new results were achieved thanks to an XRT specifically built for CAST and improved low-noise X-ray detectors.

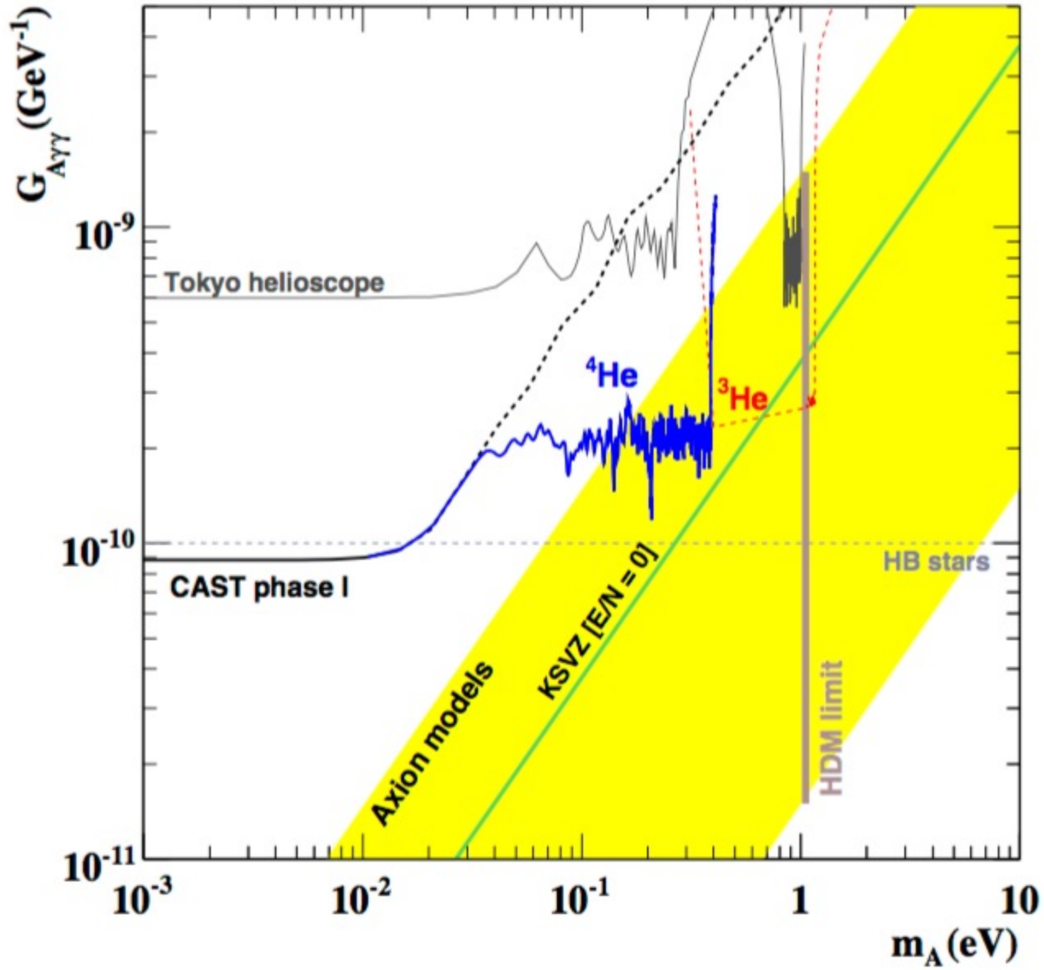

Figure 2: Solar exclusion plot for axion-like particles [50]. The red dashed line is the sensitivity of the ongoing ^{3}He phase of CAST. The vertical line (HDM) is the hot dark-matter limit [59]. The yellow band represents models with $0.07 < |E/N - 1.92| < 0.7$, the green solid line corresponds to KSVZ axions.

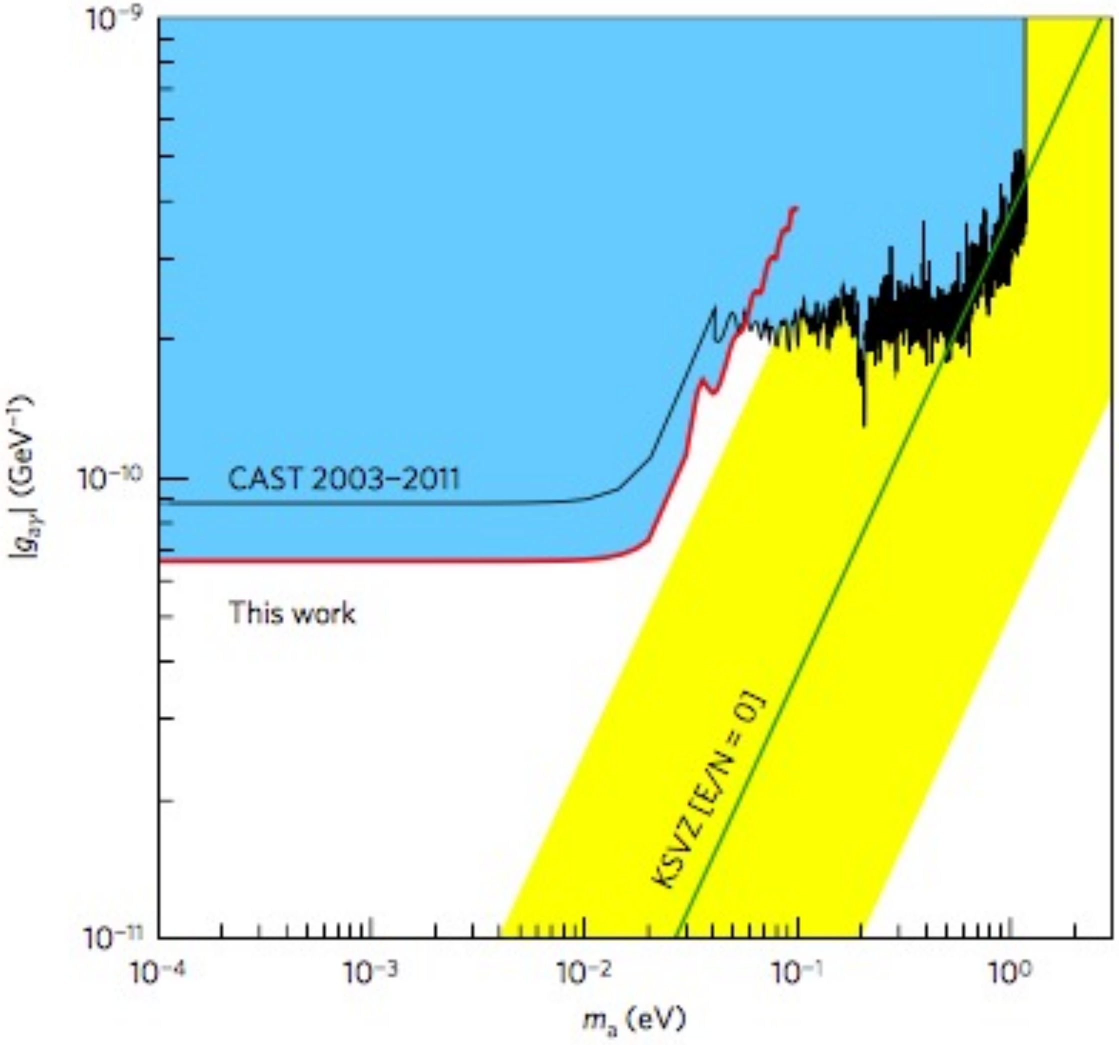

Figure 2 | CAST excluded region (95% CL) in the m_a–$g_{a\gamma}$-plane. Solid black line: Envelope of all CAST results from 2003-2011 data[11-16]. Solid red line: Exclusion from the data here presented. Diagonal yellow band: Typical QCD axion models (upper and lower bounds set according to a prescription given in ref. 49). Diagonal green line: The benchmark KSVZ axion model with $E/N = 0$, where $g_{a\gamma} = (E/N - 1.92)\alpha/(2\pi f_a)$, with f_a the axion decay constant.

Nature Physics (2017).
DOI: 10.1038/nphys4109

IAXO

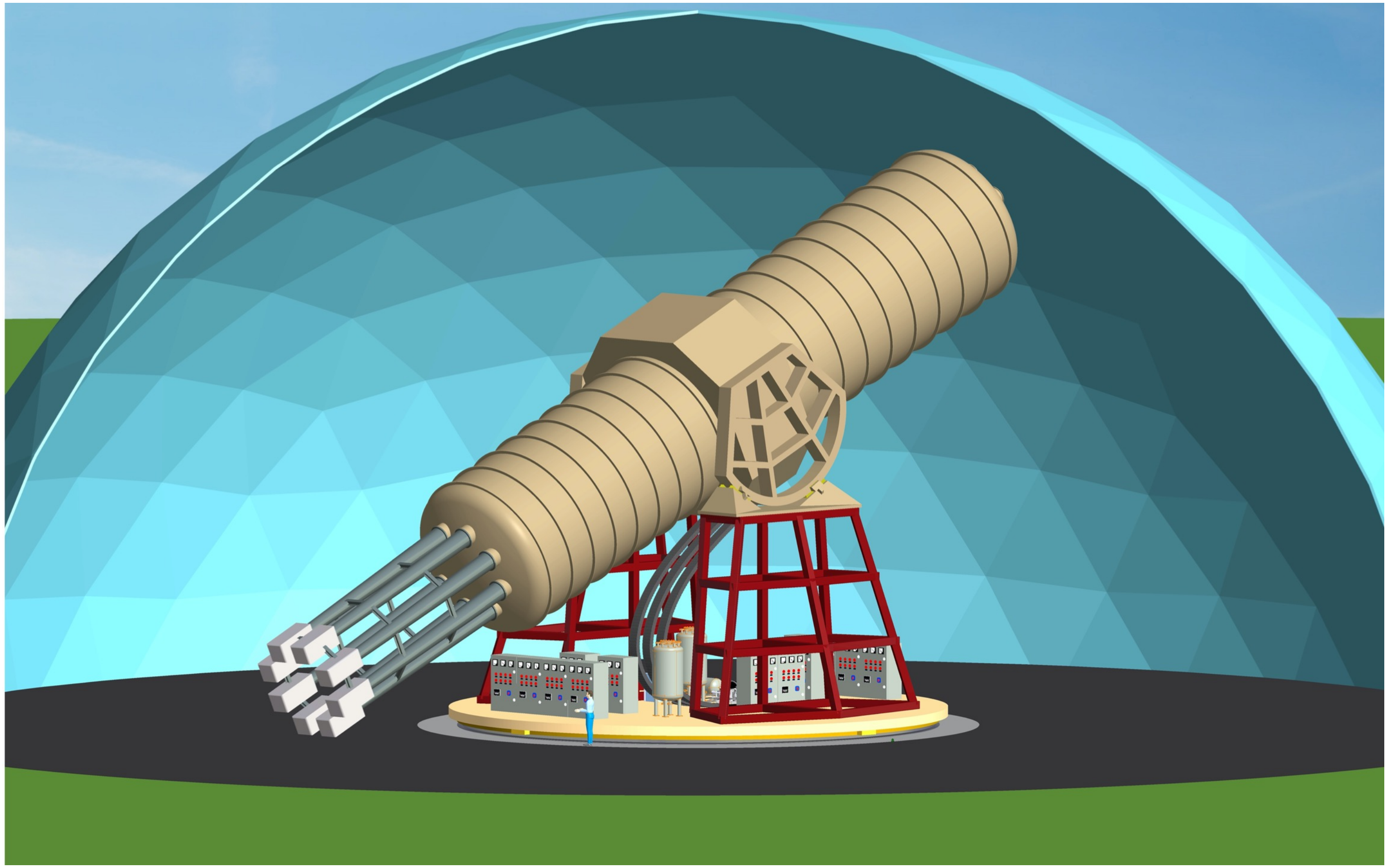

Solar axion detection concept

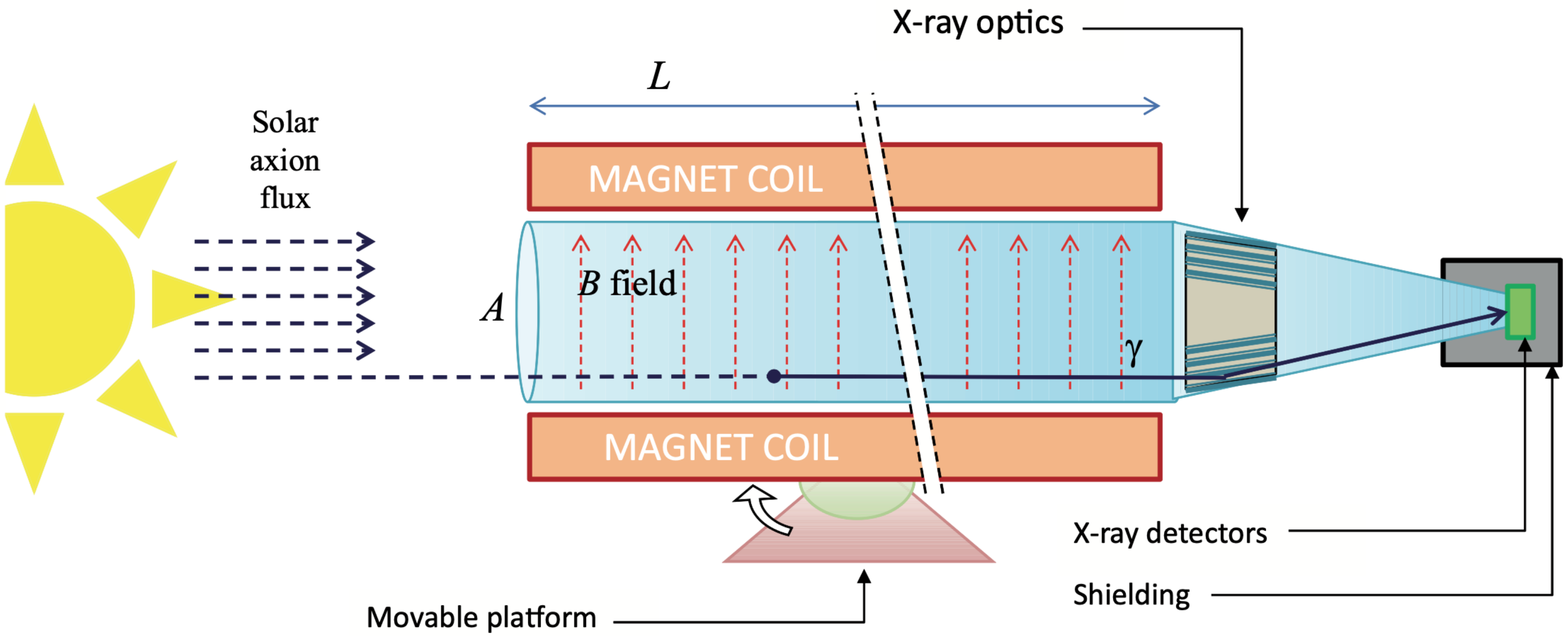

$$f \equiv f_M \, f_{DO} \, f_T$$

$$f_M = B^2 \, L^2 \, A \qquad f_{DO} = \frac{\epsilon_d \, \epsilon_o}{\sqrt{b \, a}} \qquad f_T = \sqrt{\epsilon_t \, t} \, ,$$

a: spot area
b: back ground

Parameter	Units	CAST-I	IAXO Nominal	IAXO Enhanced
B	T	9	2.5	2.5
L	m	9.26	20	20
A	m^2	2×0.0015	2.3	2.3
f_M^*		1	300	300
b	$\frac{10^{-5}\,\mathrm{c}}{\mathrm{keV\,cm^2\,s}}$	~ 4	5×10^{-3}	10^{-3}
ϵ_d		0.5 – 0.9	0.7	0.8
ϵ_o		0.3	0.5	0.7
a	cm^2	0.15	8×0.2	8×0.15
f_{DO}^*		1	17	60
ϵ_t		0.12	0.5	0.5
t	year	~ 1	3	3
f_T^*		1	3.5	3.5
f^*		1	2×10^4	6×10^4

Table 3: Values of the relevant experimental parameters representative of IAXO, both the *nominal* and *enhanced* ones, based on the considerations explained in section 4. They are compared to the ones representing the CAST vacuum phase result (CAST-I) [59]. Numbers shown for the figures of merit (equation 11) are relative to CAST-I, i. e. $f^* = f/f_{\mathrm{CAST}}$, and are approximate.

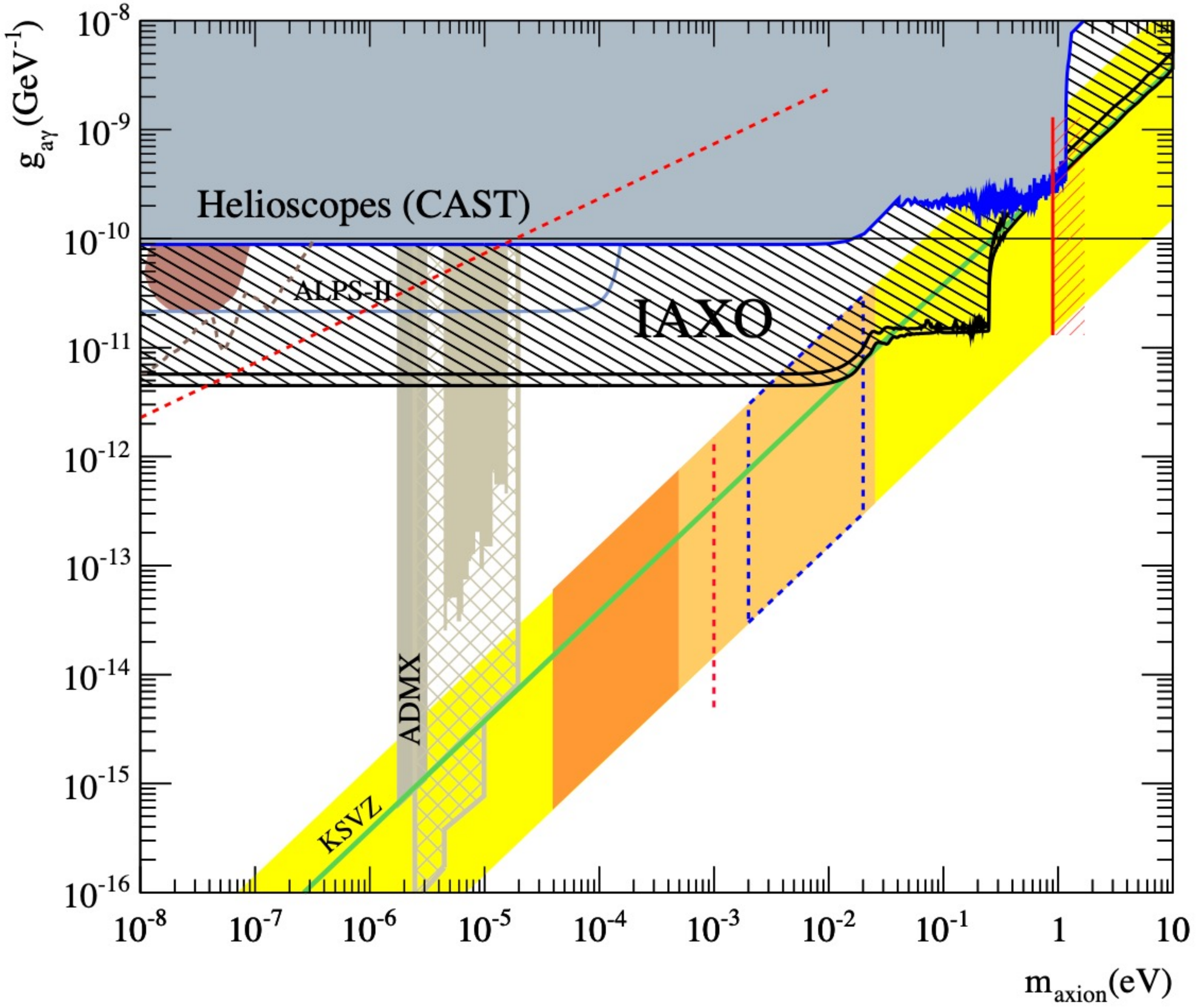

Figure 25: Expected sensitivity of IAXO as explained in the text, compared with current bounds from CAST and ADMX. Also future prospects of ADMX (dashed brown region) and ALPS-II [192] (light blue line) are shown. For the sake of clarity we have removed labels from other bounds or regions. We refer to figure 1 for those.

DM Axion search (Halo scope)

$$\mathcal{L} = -G_a \boldsymbol{E}\boldsymbol{B} a$$

$$P = \kappa g^2 V B_0^2 \rho_0 G_{lmn} \frac{1}{m_a} Q_c$$

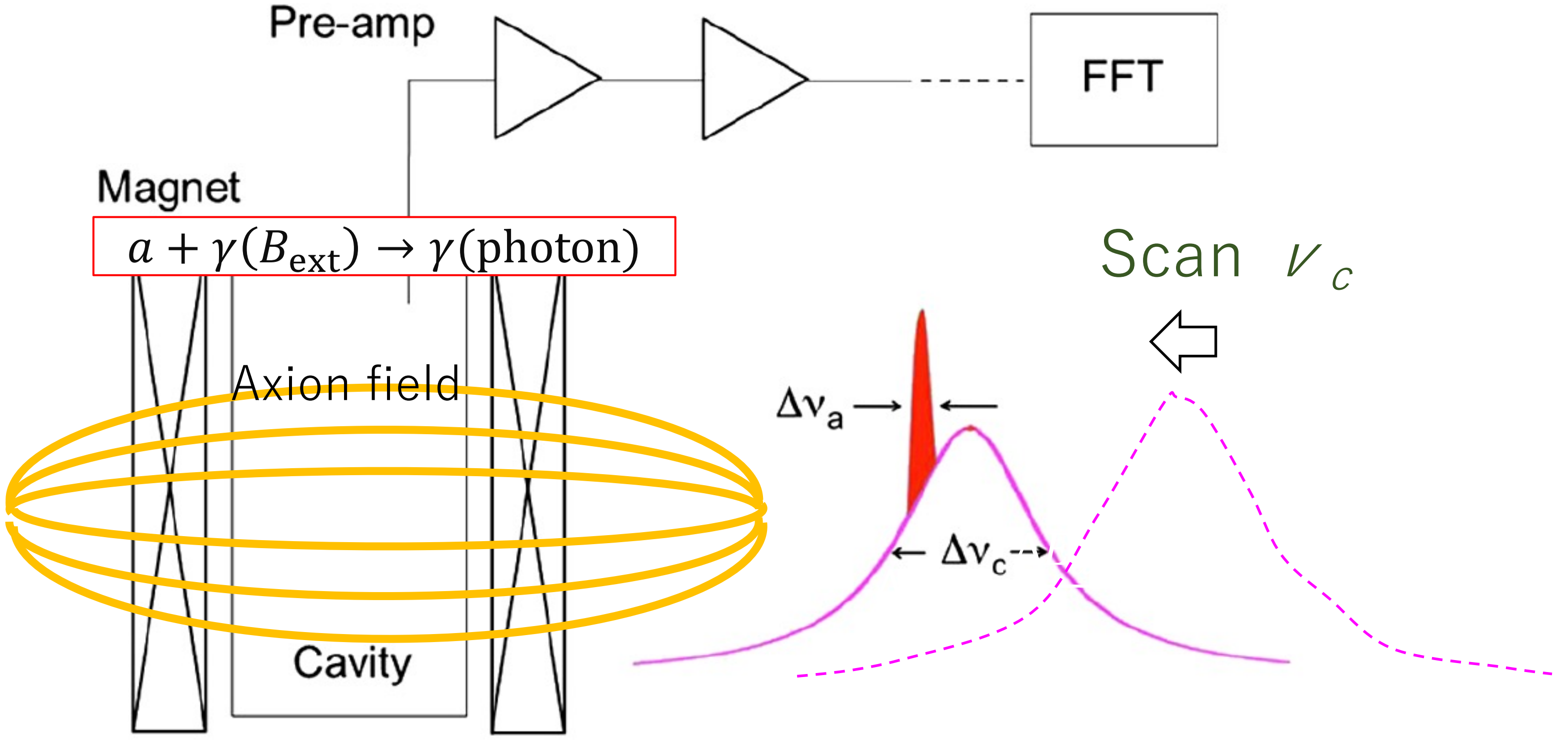

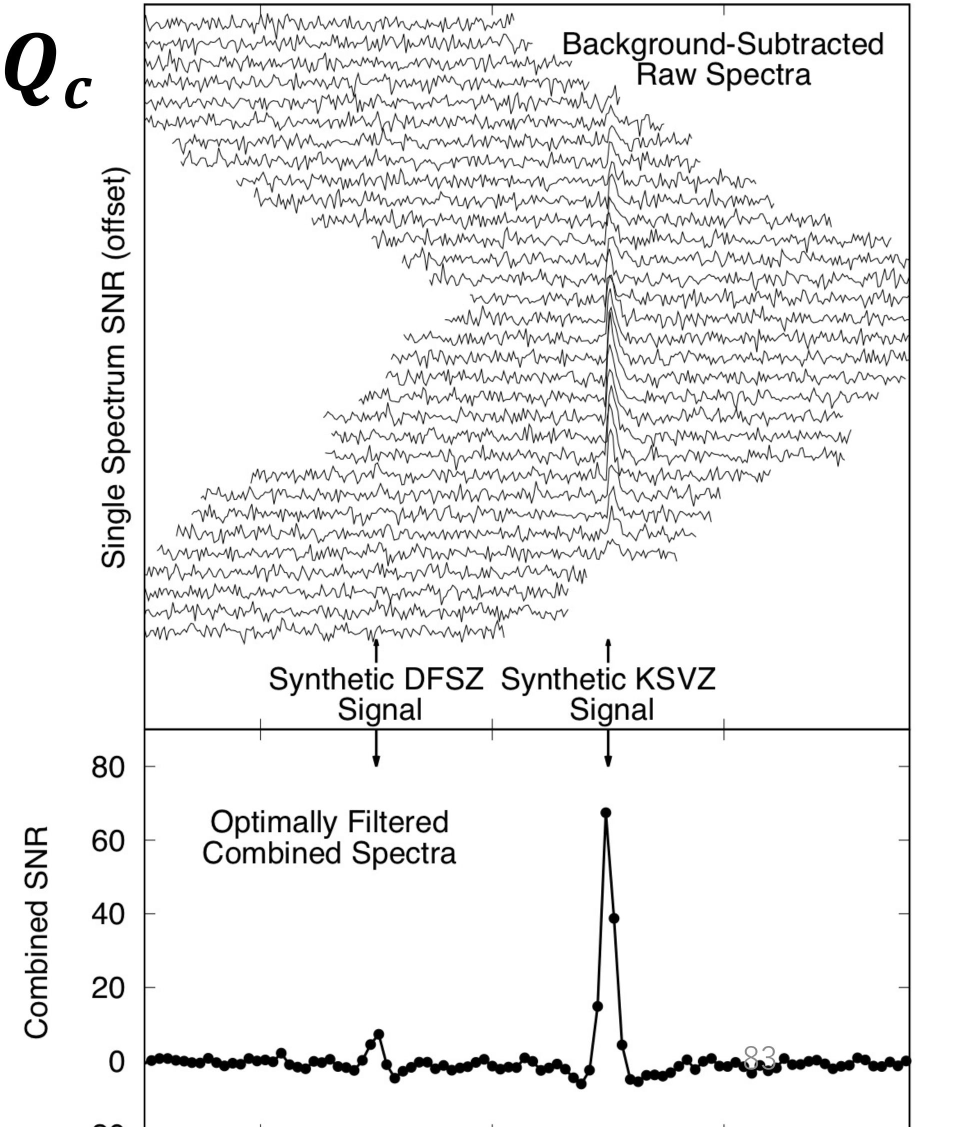

Halo scope の特徴

- 共振空洞で生じる強制振動を検出
  - $\boldsymbol{P = \kappa g^2 V B_0^2 \rho_0 G_{lmn} \frac{1}{m_a} Q_c}$
  - 信号には Q による増幅があり，熱雑音にはその増幅機能がない．
    - Q~10 5
  - 検出器のサイズは，Axion の長いde Broglie波長の半分程度が，原理的限界となる．
  - これよりキツいのが $G_{lmn} = \frac{\left(\int dV\, E_c \cdot B_0\right)^2}{|B_0|^2 V \int dV\, E_c^2}$ による制限（後述）
- Axion の質量が分からないので，それにあった共振周波数を探すことになる．
  - 宝探し．運が良い／悪いで人生が変わる

Experimental Tests of the "Invisible" Axion

P. Sikivie
Physics Department, University of Florida, Gainesville, Florida 32611
(Received 13 July 1983)

Experiments are proposed which address the question of the existence of the "invisible" axion for the whole allowed range of the axion decay constant. These experiments exploit the coupling of the axion to the electromagnetic field, axion emission by the sun, and/or the cosmological abundance and presumed clustering of axions in the halo of our galaxy.

PACS numbers: 14.80.Gt, 11.30.Er, 95.30.Cq

$$\mathfrak{L} = -\tfrac{1}{4}F_{\mu\nu}F^{\mu\nu} + \frac{e^2N}{12\pi^2}\frac{a}{v}F_{\mu\nu}\tilde{F}^{\mu\nu} + \tfrac{1}{2}\partial_\mu a\partial^\mu a - \tfrac{1}{2}m_a{}^2a^2[1+O(a^2/v^2)],$$

where $\tilde{F}^{\mu\nu} = \frac{1}{2}\epsilon^{\mu\nu\alpha\beta}F_{\alpha\beta}$, $F_{\alpha\beta} = \partial_\alpha A_\beta - \partial_\beta A_\alpha$, and where we have assumed grand unification of the strong and electroweak interactions with the unrenormalized $\sin^2\theta_w{}^0 = \frac{3}{8}$. The action density (4) has

$$\nabla\cdot\vec{E} = \frac{e^2N}{3\pi^2 v}\vec{B}\cdot\nabla a, \quad \nabla\times\vec{B} - \frac{\partial\vec{E}}{\partial t} = \frac{e^2N}{3\pi^2 v}\left[\vec{E}\times\nabla a - \vec{B}\frac{\partial a}{\partial t}\right], \quad \Box a = \frac{e^2N}{3\pi^2 v}\vec{E}\cdot\vec{B} - m_a{}^2 a.$$

Maxwell eqn. in Vac.

- $\boldsymbol{\nabla} \cdot \boldsymbol{E} = 0$
- $\boldsymbol{\nabla} \cdot \boldsymbol{B} = 0$
- $\boldsymbol{\nabla} \times \boldsymbol{B} = \frac{\partial}{\partial t} \boldsymbol{E}$
- $\boldsymbol{\nabla} \times \boldsymbol{E} = -\frac{\partial}{\partial t} \boldsymbol{B}$

With Axion

- $\boldsymbol{\nabla} \cdot \boldsymbol{E} = \kappa\, \boldsymbol{B} \cdot \boldsymbol{\nabla} a$
- $\boldsymbol{\nabla} \cdot \boldsymbol{B} = 0$
- $\boldsymbol{\nabla} \times \boldsymbol{B} = \frac{\partial}{\partial t} \boldsymbol{E} + \kappa(\boldsymbol{E} \times \boldsymbol{\nabla} a - \boldsymbol{B} \frac{\partial a}{\partial t})$
- $\boldsymbol{\nabla} \times \boldsymbol{E} = -\frac{\partial}{\partial t} \boldsymbol{B}$

- $\left(\frac{\partial^2}{\partial t^2} - \Delta\right) a + m^2 a = \kappa \boldsymbol{E} \cdot \boldsymbol{B}$
- $\kappa = \frac{e^2 N}{3\pi v}$

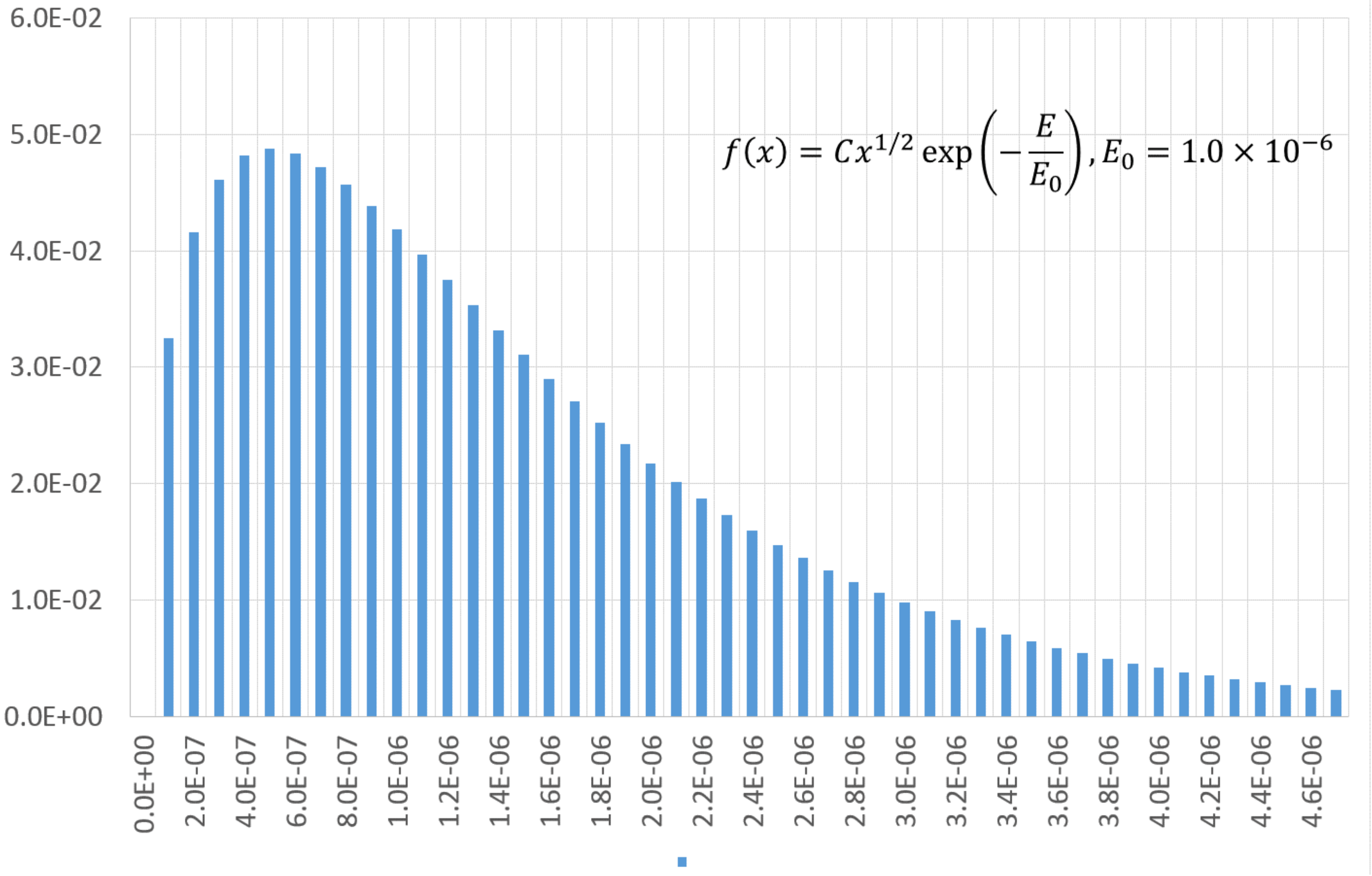

- $\Delta E = \frac{1}{2} m_a \beta^2 \sim 10^{-6} m_a$
- Spectrum may be measured with bandwidth $B \sim \frac{1}{4}\Delta E$.
  - $Q_c \sim \frac{4}{\Delta E} \sim \frac{8}{\beta^{-2}} \sim 10^7$

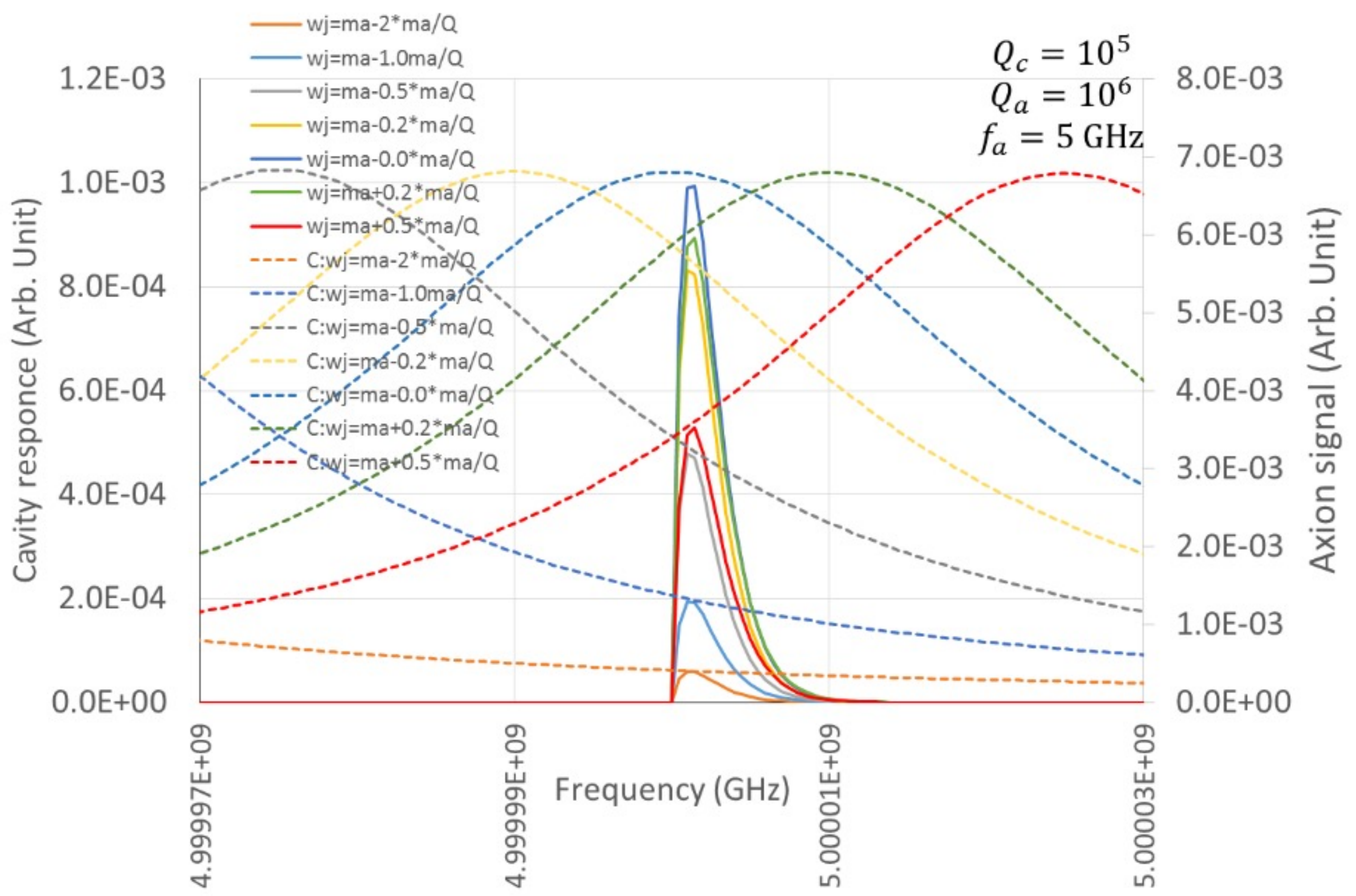

wj=ma-2*ma/Q
wj=ma-1.0ma/Q
wj=ma-0.5*ma/Q
wj=ma-0.2*ma/Q
wj=ma-0.0*ma/Q
wj=ma+0.2*ma/Q
wj=ma+0.5*ma/Q
C:wj=ma-2*ma/Q
C:wj=ma-1.0ma/Q
C:wj=ma-0.5*ma/Q
C:wj=ma-0.2*ma/Q
C:wj=ma-0.0*ma/Q
C:wj=ma+0.2*ma/Q
C:wj=ma+0.5*ma/Q
$Q_c = 10^5$
$Q_a = 10^6$
$f_a = 5$ GHz
Cavity responce (Arb. Unit)
Axion signal (Arb. Unit)
Frequency (GHz)
1.2E-03
1.0E-03
8.0E-04
6.0E-04
4.0E-04
2.0E-04
0.0E+00
8.0E-03
7.0E-03
6.0E-03
5.0E-03
4.0E-03
3.0E-03
2.0E-03
1.0E-03
0.0E+00
4.99997E+09
4.99999E+09
5.00001E+09
5.00003E+09

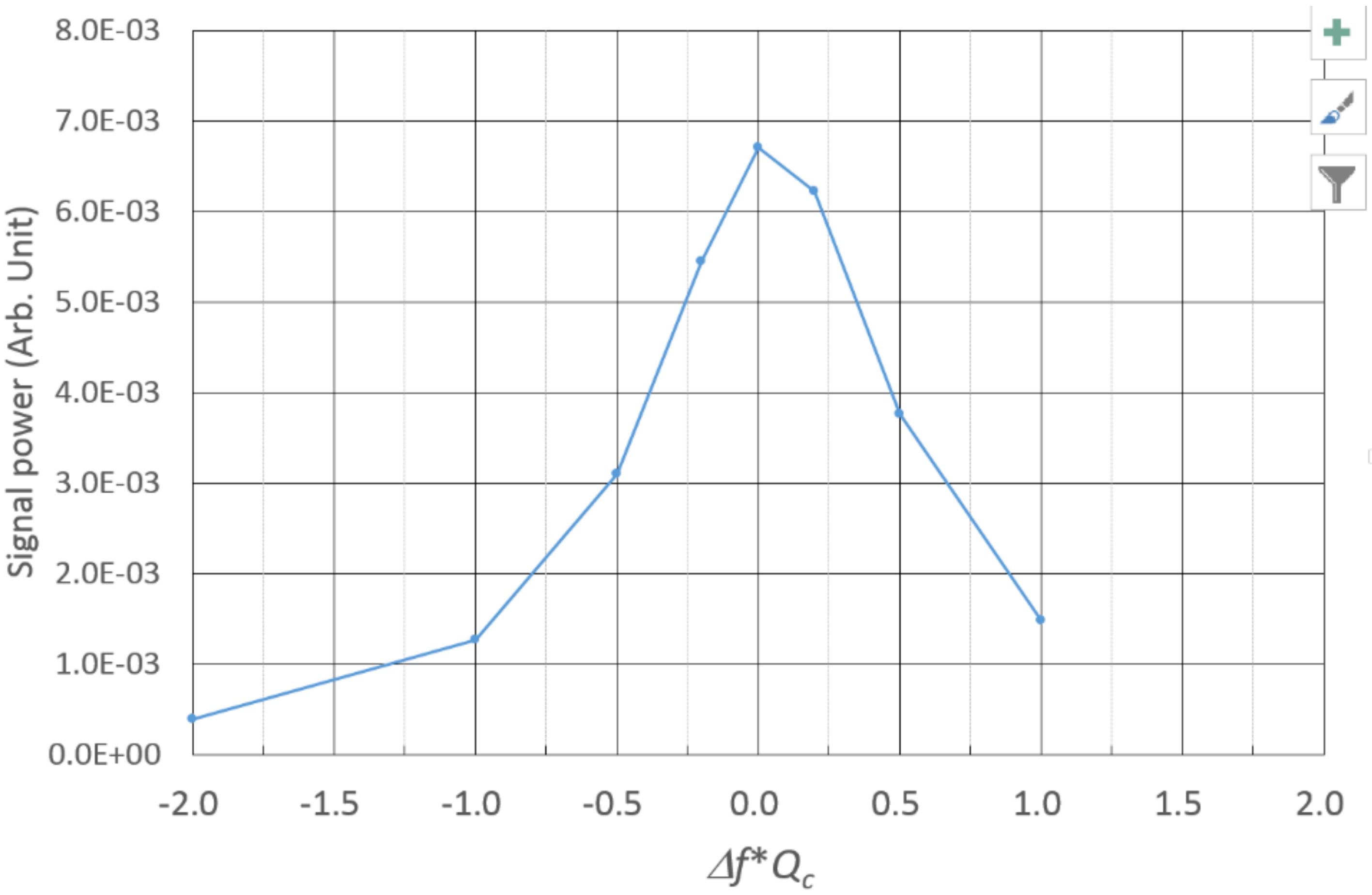

Qを単位にScanするのは荒すぎる.
0.2Q位が適切.

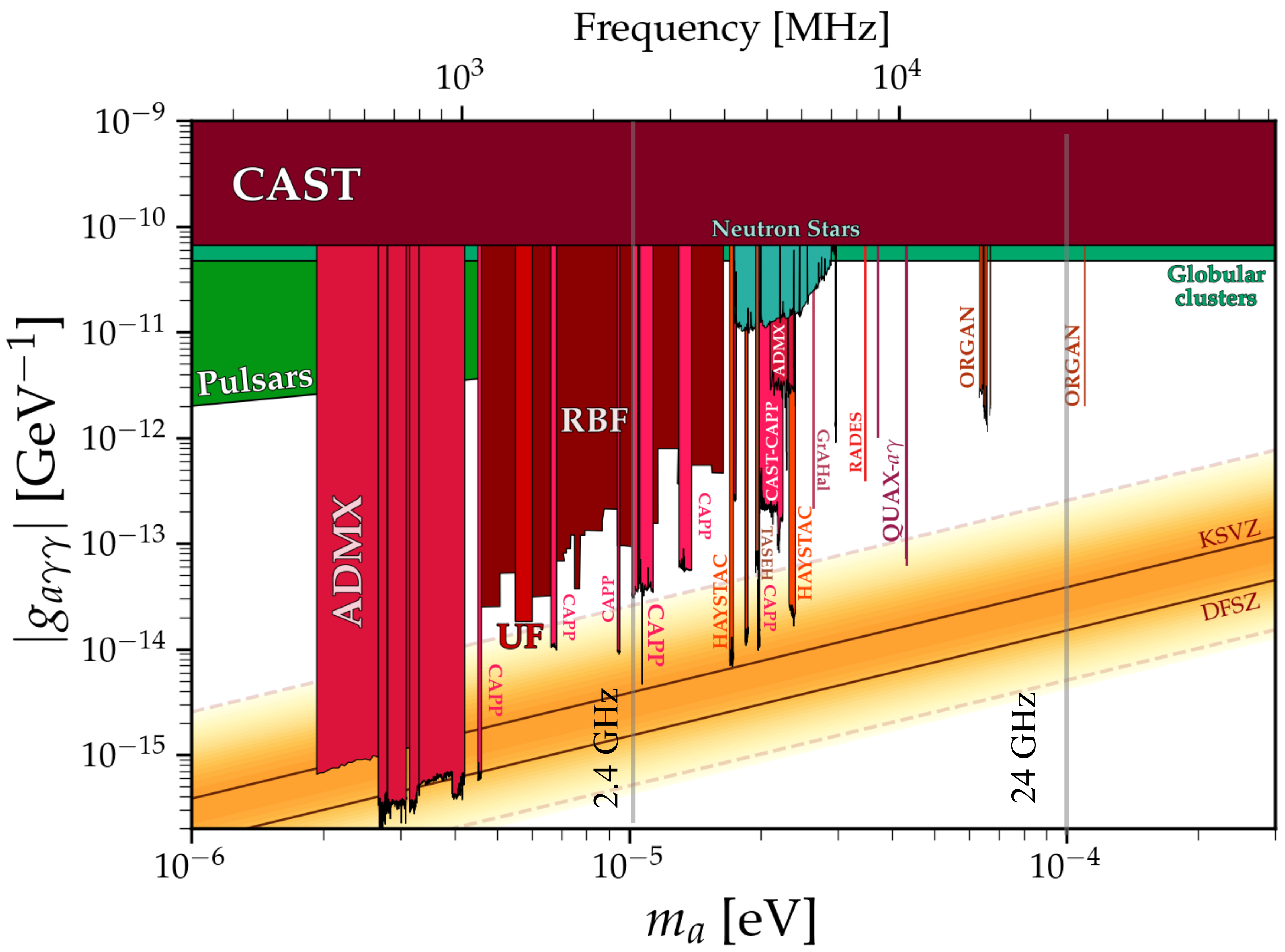
Frequency [MHz]
10^3
10^4
10^{-9}
10^{-10}
10^{-11}
10^{-12}
10^{-13}
10^{-14}
10^{-15}
$|g_{a\gamma\gamma}|$ [GeV^{-1}]
CAST
Neutron Stars
Globular clusters
Pulsars
ADMX
RBF
UF
CAPP
CAST-CAPP
HAYSTAC
TASEH
GrAHal
RADES
QUAX-$a\gamma$
ORGAN
KSVZ
DFSZ
2.4 GHz
24 GHz
10^{-6}
10^{-5}
10^{-4}
m_a [eV]

ADMX 実験（世界の先頭）

- $ADMX_0$
  - f=0.3~0.5GHz
  - T=1.3K
  - T_{amp}=2.0~4.0K

- $ADMX_1$
  - f=0.8~0.9GHz
  - T=2.0K
  - T_{amp}=1.0~4.0K

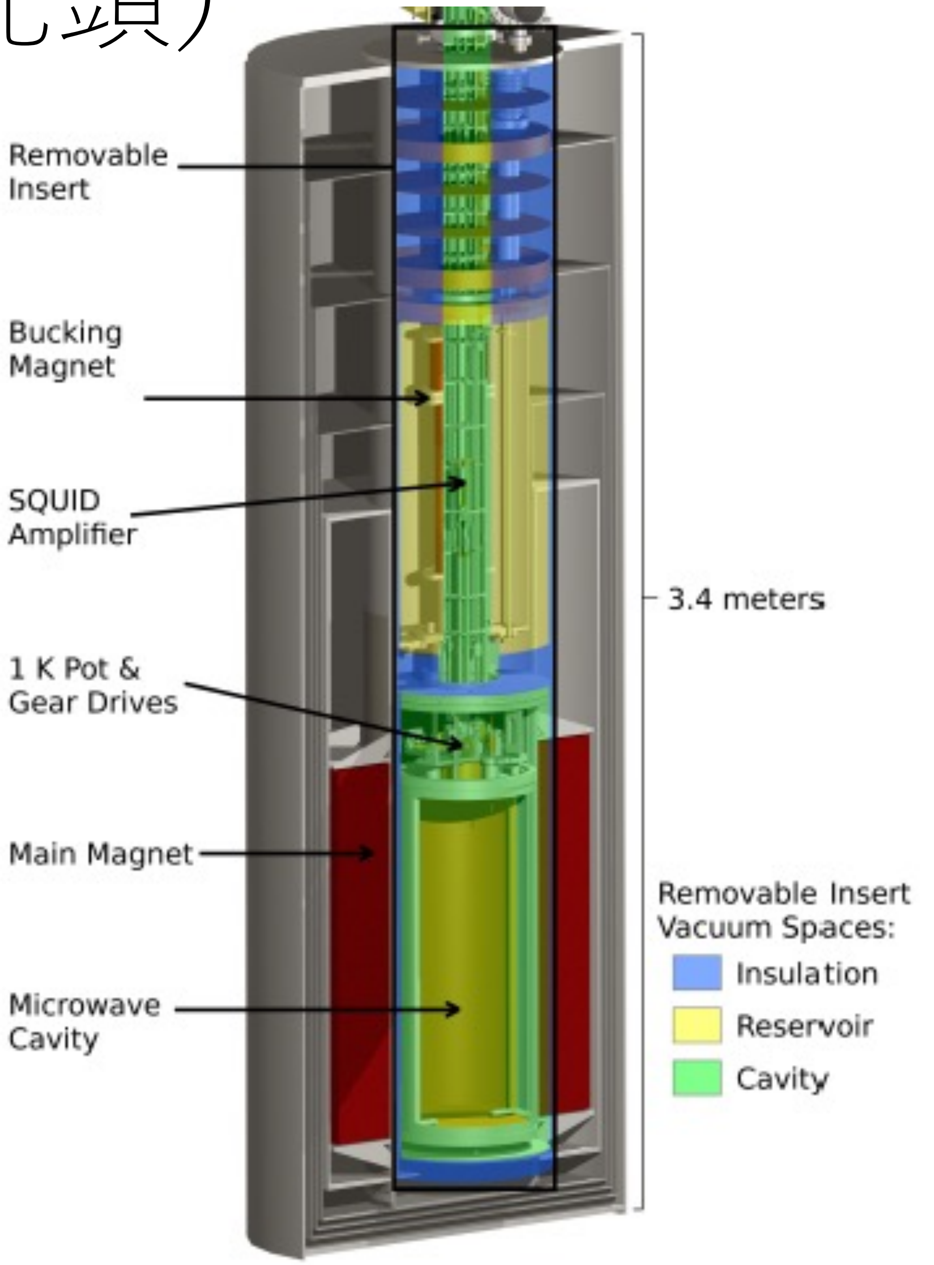

雑音が検出限界を決める.

- アンプ雑音と熱輻射光子

コンベンショナルなアンプでKSVZに到達は可能

更に上に行くには，希釈冷凍機と量子センサーを使用

●SQUID，JPA など

- Experimental issues:
  - Amplifier noise
  - Background photons
    - Blackbody radiation
    - Galactic photons
  - Cavity resonance frequency

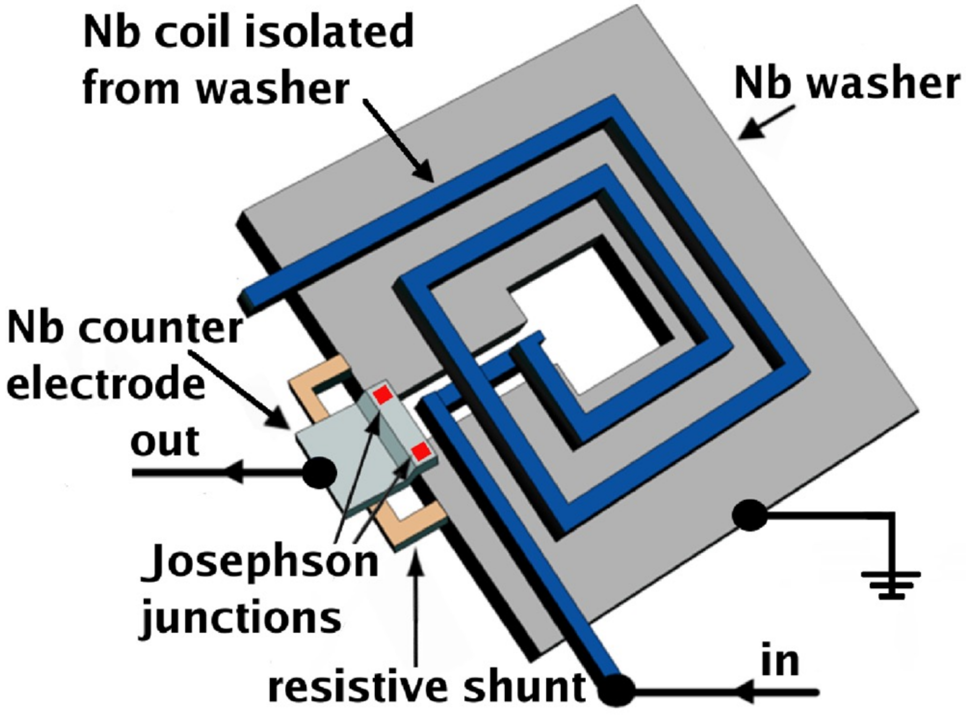

Asztalos 他 PRL 104, 041301 (2010)

Dicke radiometer

THE REVIEW OF SCIENTIFIC INSTRUMENTS VOLUME 17, NUMBER 7 JULY, 1946

The Measurement of Thermal Radiation at Microwave Frequencies

R. H. DICKE*
*Radiation Laboratory, Massachusetts Institute of Technology, Cambridge, Massachusetts***

(Received April 15, 1946)

The connection between Johnson noise and blackbody radiation is discussed, using a simple thermodynamic model. A microwave radiometer is described together with its theory of operation. The experimentally measured root mean square fluctuation of the output meter of a microwave radiometer (0.4°C) compares favorably with a theoretical value of 0.46°C. With an r-f band width of 16 mc/sec., the 0.4°C corresponds to a minimum detectable power of 10^{-16} watt. The method of calibrating using a variable temperature resistive load is described.

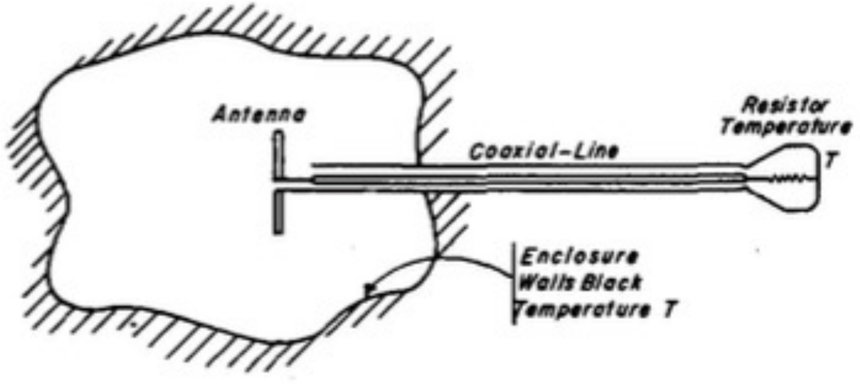

FIG. 1. Antenna system in black enclosure.

$$kT_{sys} = P_{sys}(\nu)$$

$$\sigma = \frac{T_{sys}}{\sqrt{N}} = \frac{T_{sys}}{\sqrt{\Delta f \tau}}$$

- $\frac{S}{N} = \frac{P_a}{P_n}\sqrt{\Delta\nu\ t}$
- $\quad = \frac{P_a}{kT_{sys}}\sqrt{\frac{t}{\Delta f}}$
  - Narrow band Δf
  - Longer integration t

- Signal P_a can be found with bandwidth Δf in integration time t.
  - $t = \left(\frac{S}{N}\right)^2 \left(\frac{kT_{sys}}{P_a}\right)^2 \Delta f$
  - In axion case, $\Delta f = f_a/Q_a$ and $P_a \propto Q_c$, then $t \propto Q_c^{-2}$
- If we search for axion, its mass is unknown, so assume search ΔF around f_a, the scan rate $\frac{\Delta F}{\Delta t} = \frac{\Delta F}{Q_c}\frac{1}{t} \propto Q_c$.

- Lager Q_c always helps.

- $T_{abs} = 2.725 \pm 0.002$ K
  - By FIRIS
- $\Delta T = 36 \pm 5$ μK at 7 deg.
- $\Delta T = 30.5 \pm 2.7$ μK at 10 deg.
  - By DMR

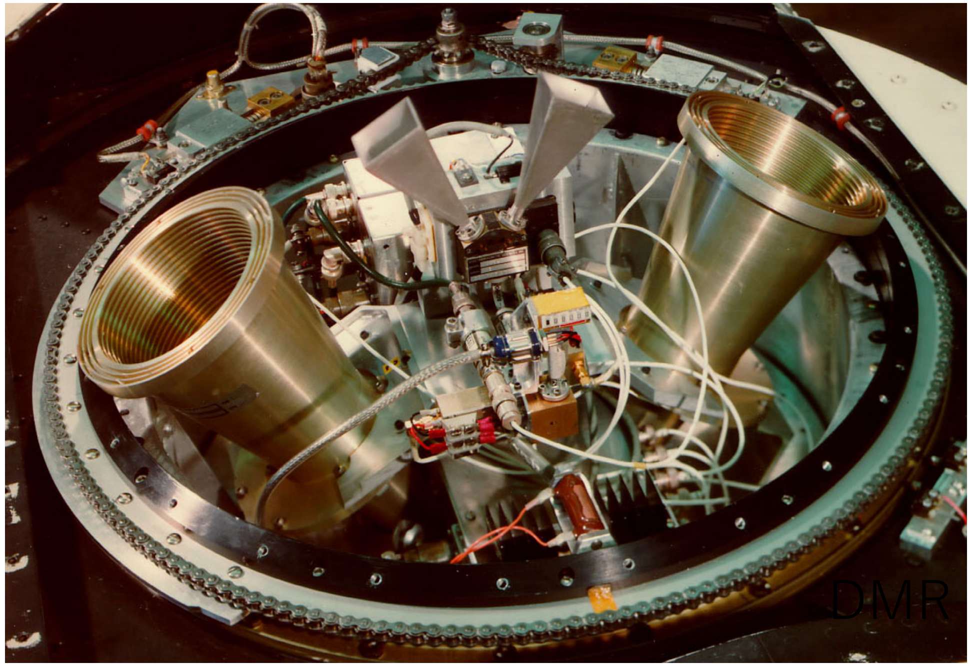

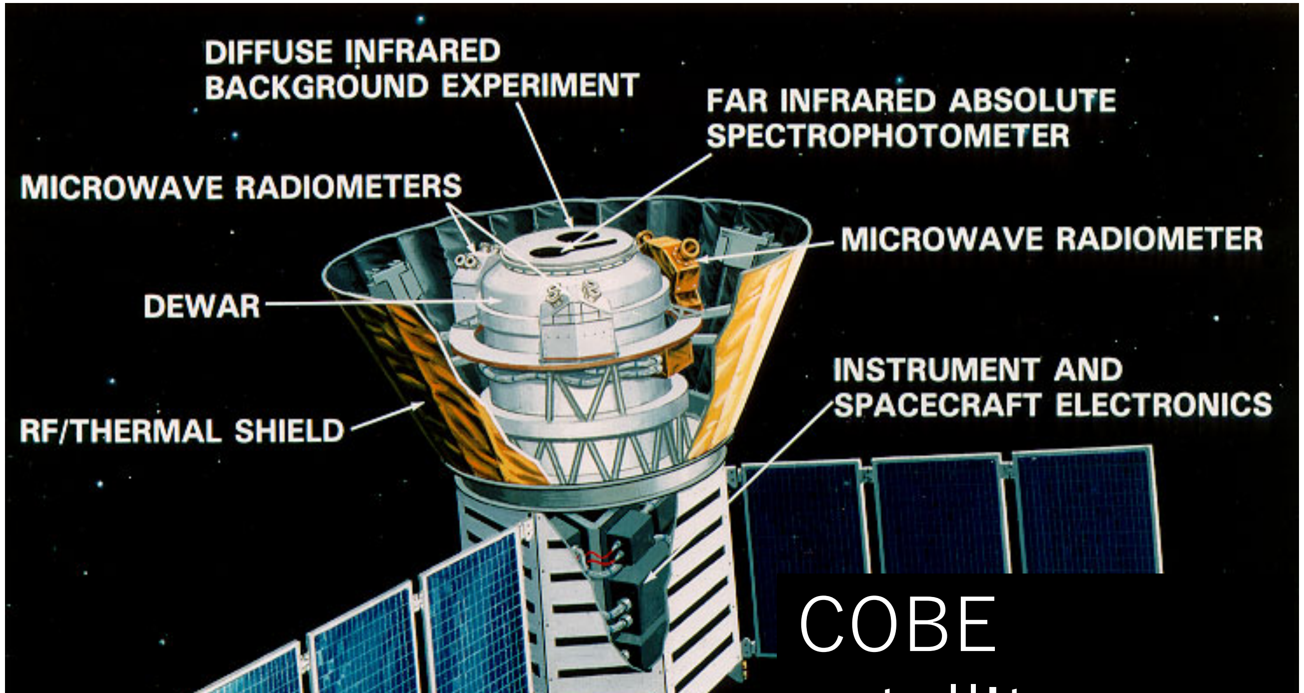

広範囲でのアクシオン探索（宝探しの場所）

低周波数側

- 空洞サイズで決まる
  - 大きなマグネットは容易でない．
- 熱雑音が厳しい
  - $g_{a\gamma\gamma}$が小さくなる上，熱雑音は $e^{-\frac{E}{kT}}$
- 質量が小さいと，Over production するが，これを逃れる理論もある．

高周波数側

- 理論サイドから，高い周波数が好まれている．
  - PDB： $m_a \approx 25\ \mu\mathrm{eV} \sim 4.4\ \mathrm{meV},\ 0.58 - 130\ \mathrm{meV}$
- $G_{lmn} = \frac{\left(\int dV\, E_c \cdot B_0\right)^2}{|B_0|^2 V \int dV\, E_c^2}$ の制約

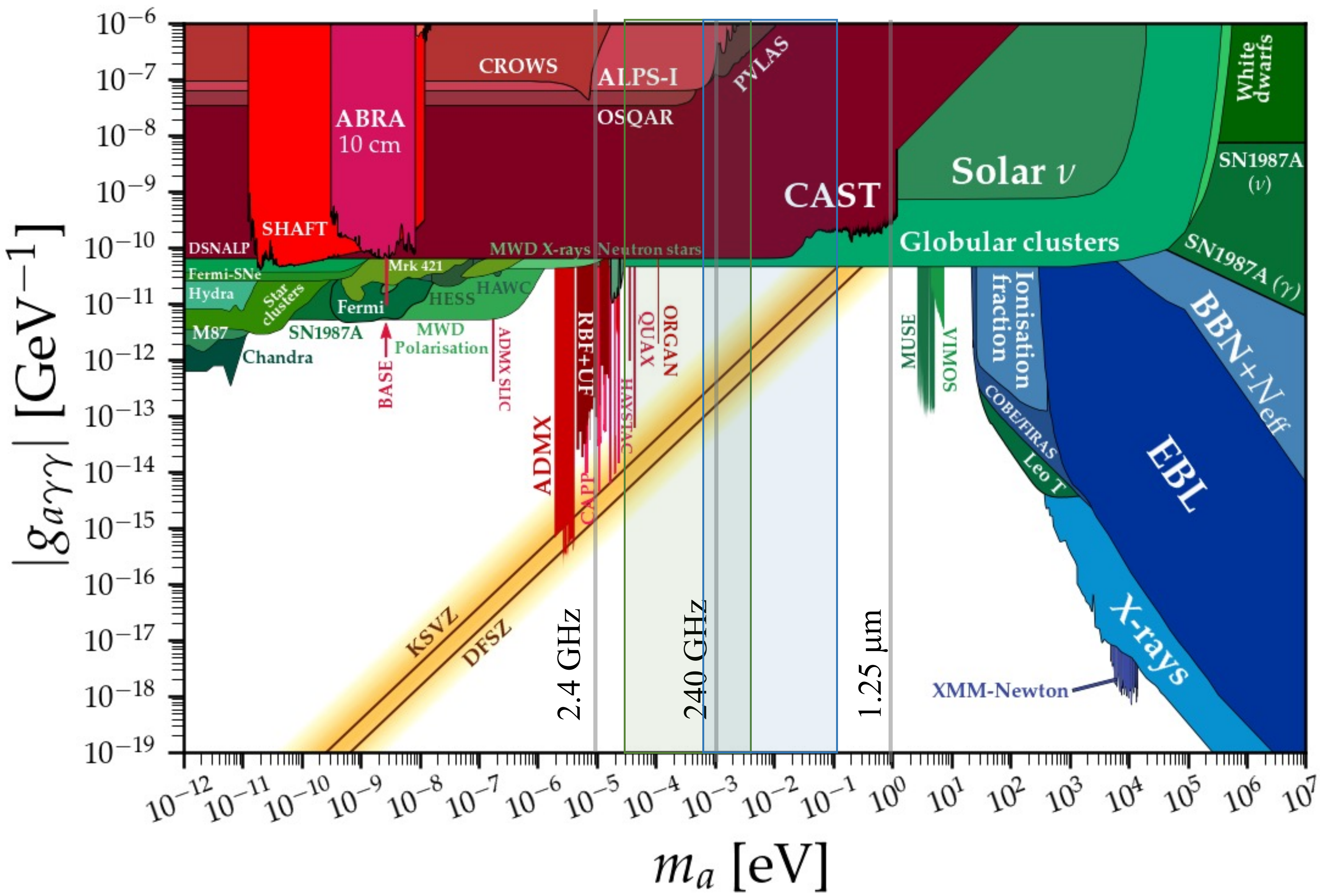

https://cajohare.github.io/AxionLimits/docs/ap.html

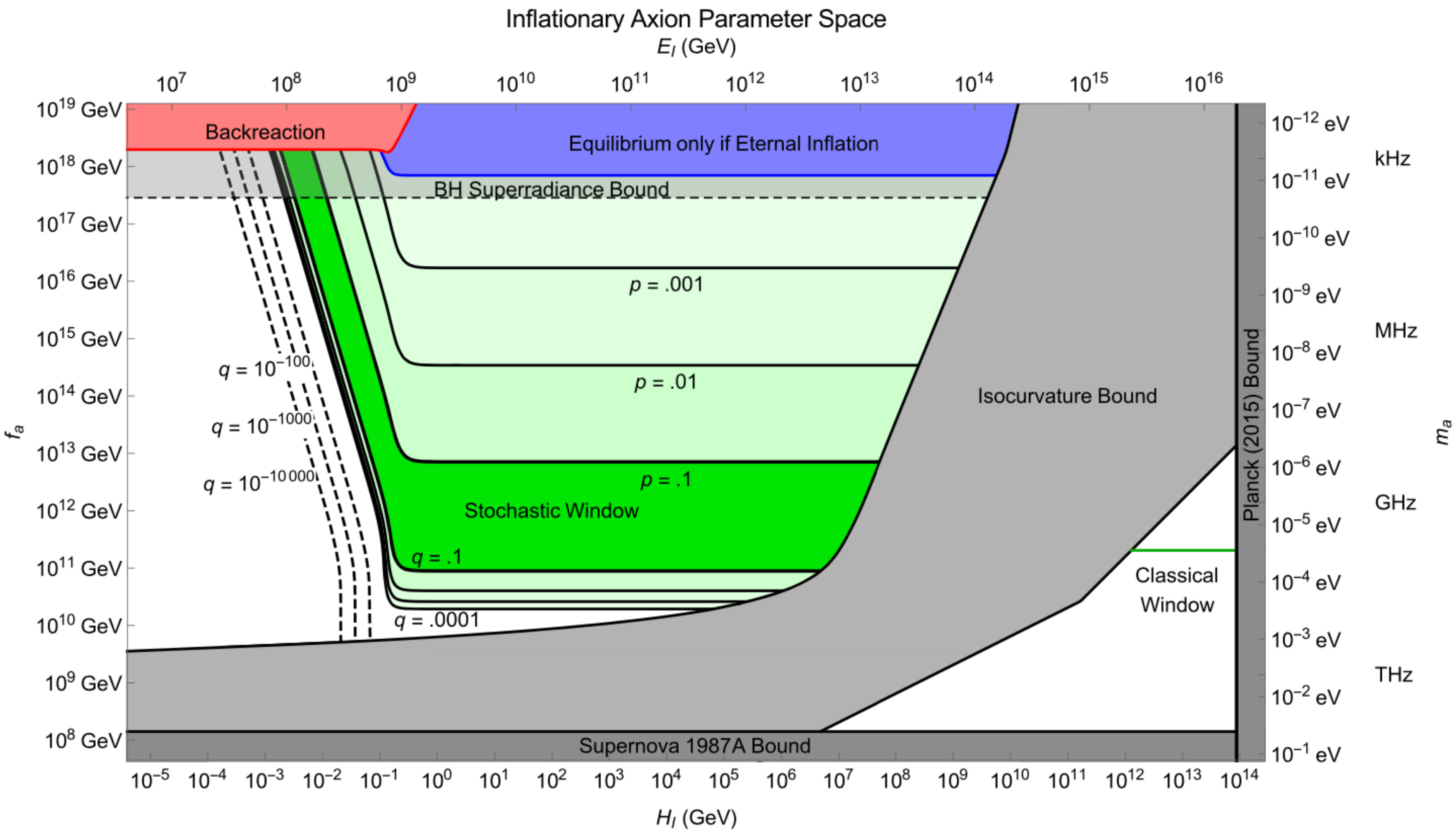

FIG. 2. Parameter space for the QCD axion dark matter, assuming a long enough period of inflation that the axion reaches equilibrium as described in the text. Axes are axion decay constant f_a (left) and mass m_a (right, inverted), Hubble scale of inflation H_I (bottom), and inflationary energy scale $E_I = (3H_I^2 M_P^2)^{1/4}$ (top). In the large green region, the observed dark matter density is a typical density to get from our axion equilibrium distribution ($p > .1$ and $q > .1$). Smaller values of p and q are shown as solid and dashed contours around this region. At near-Planckian f_a, the axion's behavior changes: in the pink region, backreaction effects become significant and force $\theta \to \pi$; in the blue region, the distribution does not reach equilibrium and depends on initial conditions, except in eternal inflation. At high H_I and low f_a is the classical window, where PQ symmetry breaks and produces axions after inflation. The thin green line shows the standard value of f_a where this production matches the observed dark matter density. Observational constraints are shown in gray: isocurvature from the CMB spectrum, a lower bound on f_a from supernova 1987A, black-hole superradiance, and an upper bound on H_I from the Planck 2015 constraint on r.

Dish antenna

$$a + \gamma(B_{\mathrm{ext}}) \to \gamma(\mathrm{photon})$$

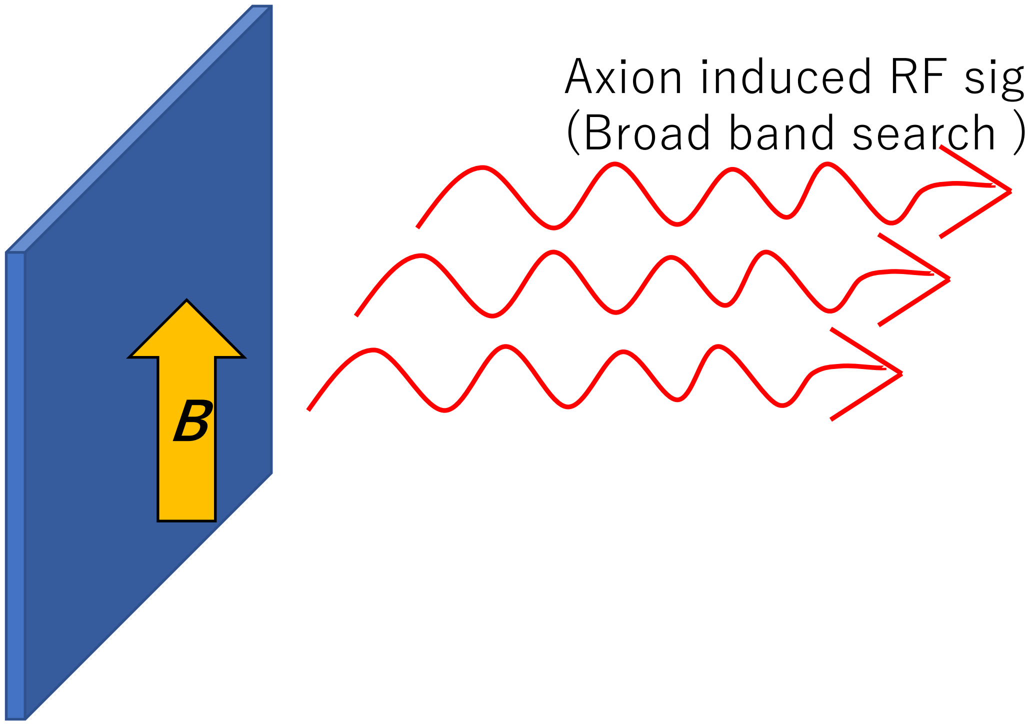

Dish antenna

$$\boldsymbol{P_{Dish} = \kappa g^2 B_0^2 \rho_0 \frac{1}{m_a^2} A}$$

Halo scope

$$\boldsymbol{P_{HS} = \kappa g^2 V B_0^2 \rho_0 G_{lmn} \frac{1}{m_a} Q_c}$$

$$Q_c \approx {}^{A}/_{\lambda_a^2} \sim 10^4 \left({}^{A\,(\mathrm{m}^2)}/_{\lambda\,(\mathrm{cm})}\right) = 10^4 (A(m^2)) \frac{\nu\,(\mathrm{GHz})}{30\ \mathrm{GHz}},$$

Many project to search for axion

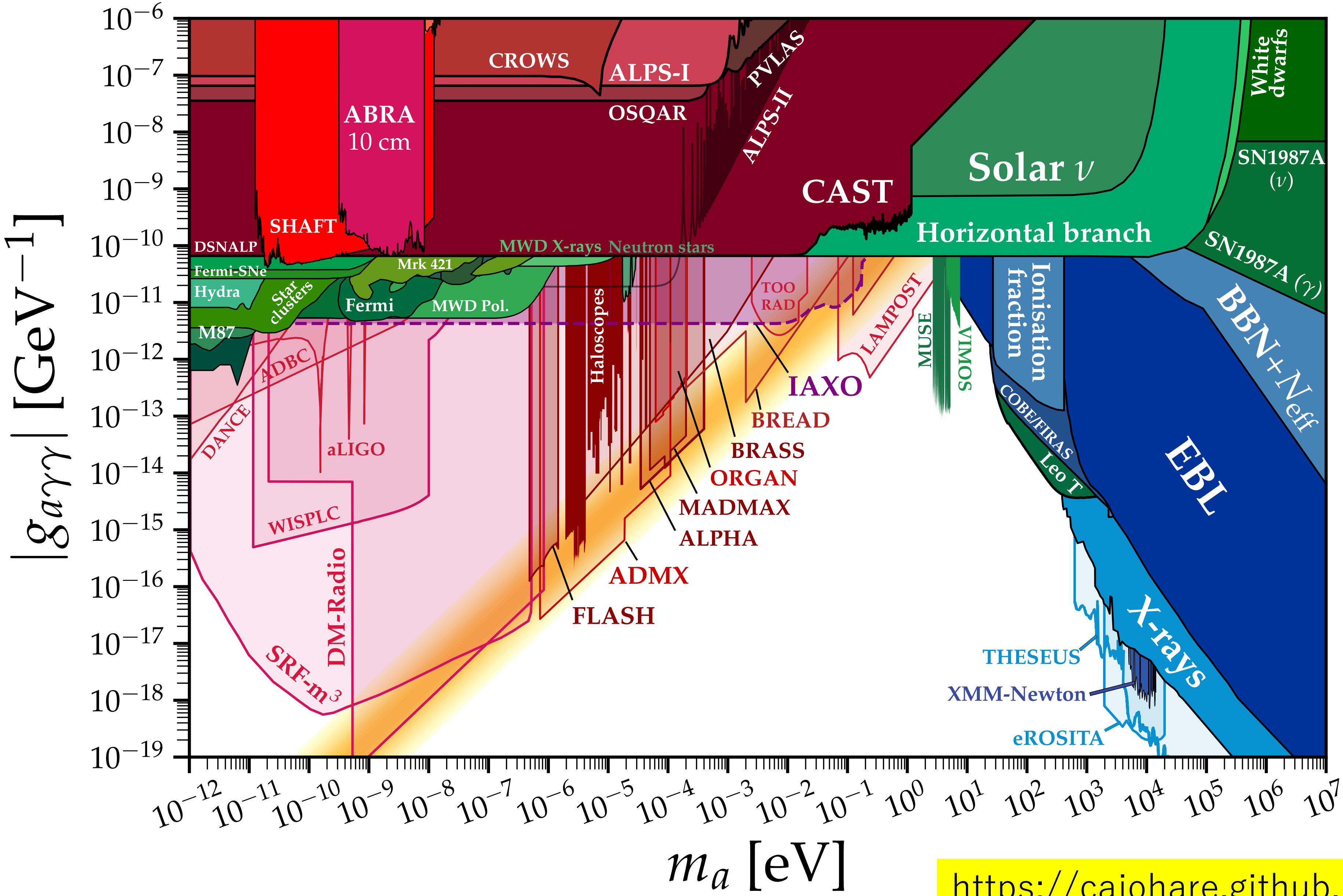

https://cajohare.github.io/AxionLimits/

ＡＬＰ と ＨＰ

- 実験的には
  - ＡｘｉｏｎとＡＬＰは原理的には同じ
  - ＨＰは磁場なしでＯＫ
- 理論的には,
  - ＡｘｉｏｎはＱＣＤ
  - ＡＬＰｓとＨＰはＳｔｒｉｎｇ
    - 10次元時空を4次元にコンパクト化する際にストリングアクシオンが現れる.
    - 典型的には $f_a \sim 10^{16}\ \mathrm{GeV}$
    - 光子と結合するものを ALPs と呼ばれる
    - ＨＰは，軽いＵ（１）が出る理論

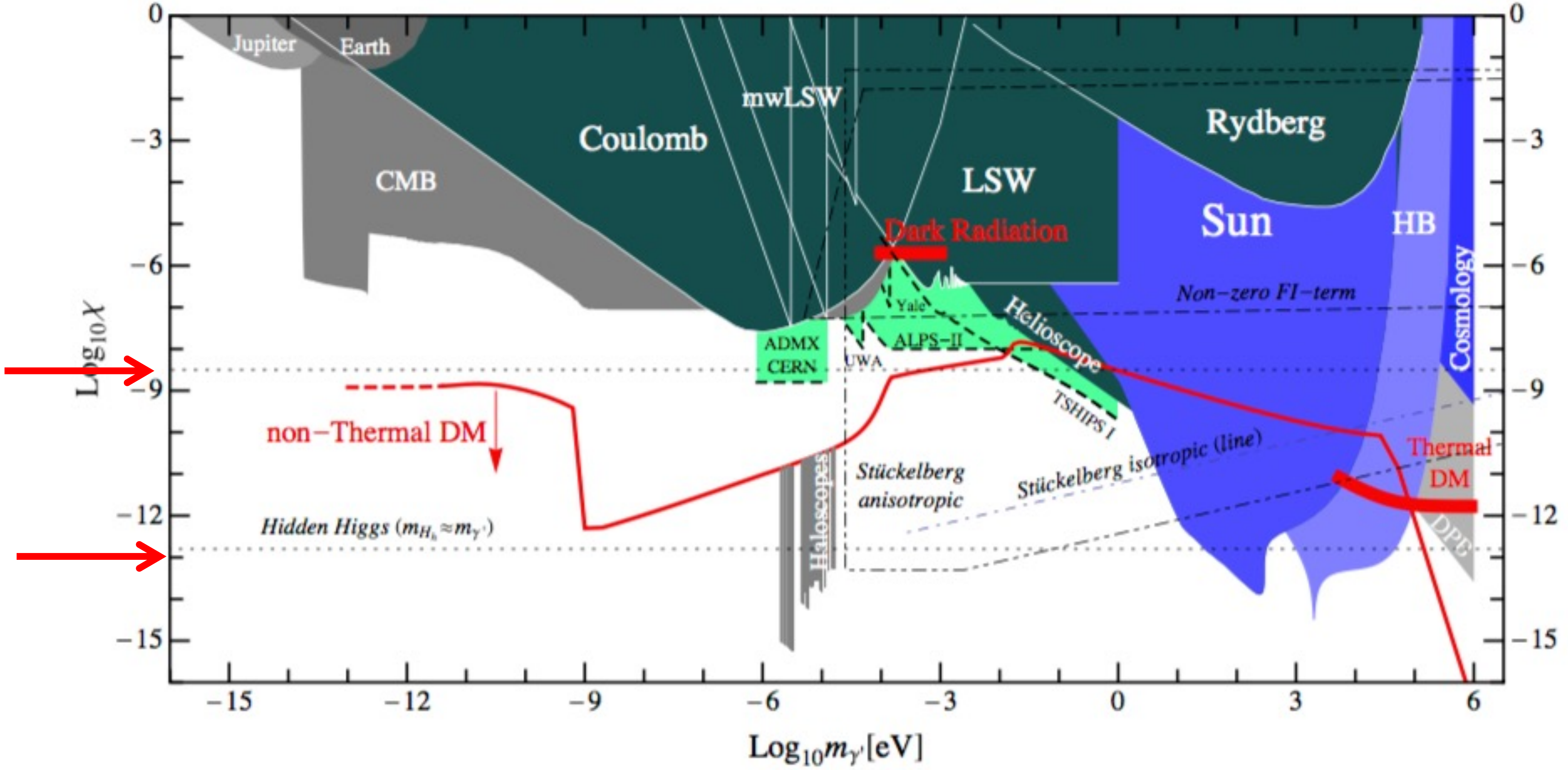

Fig. 4. Kinetic mixing parameter vs. hidden photon mass (adapted from Refs. [2,3,27]). Coloured regions are: experimentally excluded regions (dark green), constraints from astronomical observations (grey) or from astrophysical or cosmological arguments (blue), and sensitivity of planned experiments (light green). Shown in red are boundaries where the hidden photon would account for all cold dark matter produced either thermally or non-thermally by the vacuum-realignment mechanism or where the hidden photon could account for the hint of dark radiation during the CMB epoch. The regions bounded by dotted lines show predictions from string theory corresponding to different possibilities for the nature of the hidden photon mass: Hidden-Higgs, a Fayet-Iliopoulos term, or the Stückelberg mechanism. In general, predictions are uncertain by factors of order one. (For interpretation of the references to colour in this figure legend, the reader is referred to the web version of this article.)

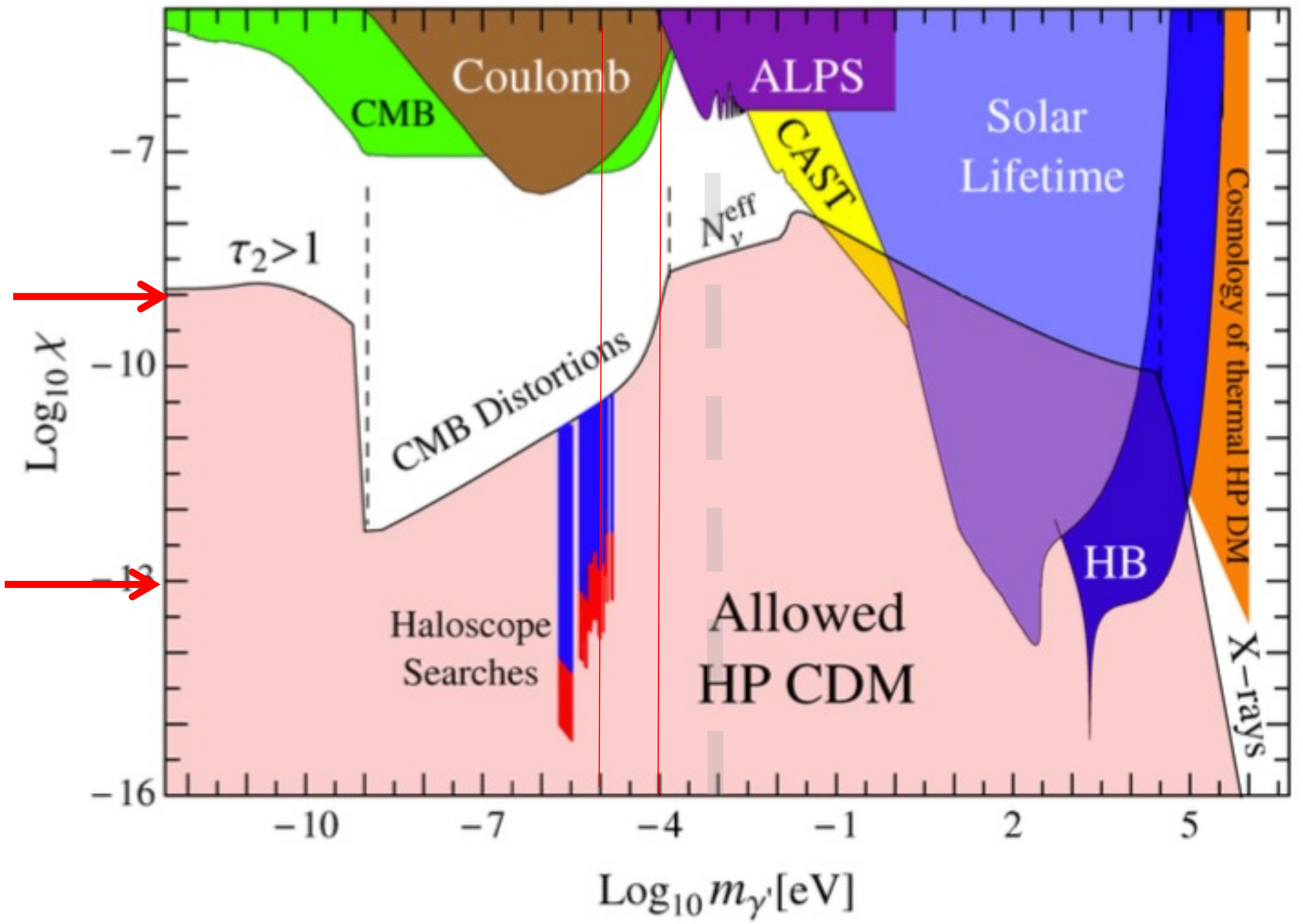

Figure 5. Allowed parameter space for hidden photon cold dark matter (HP CDM) (for details see text). The exclusion regions labelled "Coulomb", "CMB", "ALPS", "CAST" and "Solar Lifetime" arise from experiments and astrophysical observations that do not require HP dark matter (for a review see [38]). We also show constraints on the "cosmology of a thermal HP DM". Note that only constraints on HPs with masses below twice the electron mass are shown since otherwise the cosmological stability condition requires unreasonably small values of the kinetic mixing, χ. The four constraints that bound the allowed region from above, "$\tau_2 > 1$", "CMB distortions", "$N_\nu^{\rm eff}$" and "X-rays" are described in the text.

まとめ

- 暗黒物質についての基礎的な事柄
  - どこにどんな風にあるのか
- Axion
  - 実験的探索の原理など
- Axionの他（ALPsとHP）